PAP-763

GCID Model Study
Progress Report
Screen Model and Fish Bypass Model

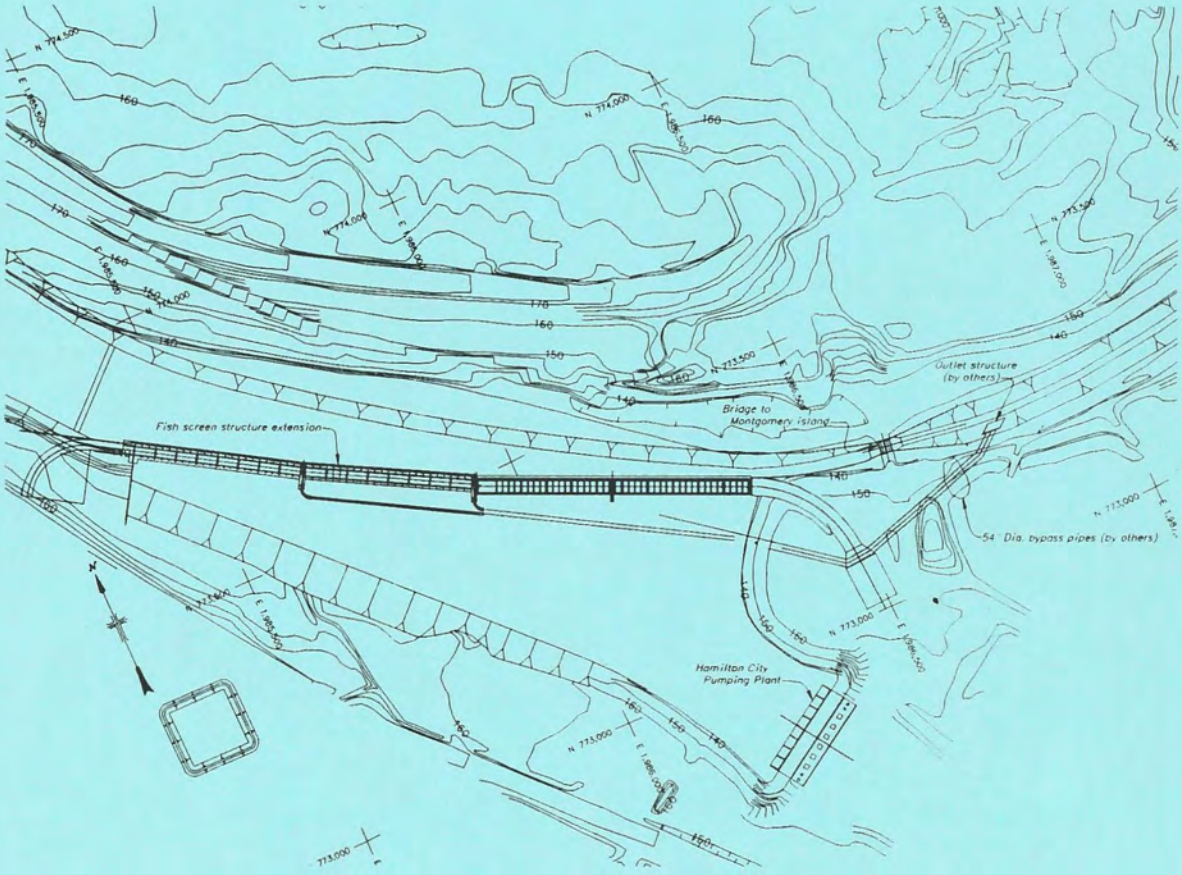

Progress Report - GCID Physical Model Studies
Structure Design with Three Fish Bypasses and a Gradient Restoration Structure
April 1997
Brent Mefford

Two physical models are currently being tested to assist in the final design of the GCID fish screen structure. Testing of the final design fish screen layout was completed in the 1:16 scale fish screen model. In addition, a 1:5 scale model of an internal fish bypass was constructed and tested. Progress results of both studies are included herein.

Screen Model

The screen layout was changed after the decision by the TAG to focus on a screen structure with three internal fish bypasses, a gradient restoration structure (referred to as GF2) in the main river, and a check structure in the lower oxbow downstream of the screen. Bypasses needed to be positioned at the bend points in the screen alignment and set at approximate equal intervals along the screen face. To accomplish this, the upstream-most screen angle was moved to the mid-point of the new screen (~288 ft from the end), and the screen deflection angle was reduced from 4° to 2.9°, figure 1. The changes to the screen layout did not alter the end positions of the new screen compared to the previous design. The location of the fish bypass in the existing screen was positioned at the mid-point of the screen. Oxbow flows and water surface elevations used in the physical model tests are given in Table 1. The data are based on 2-dimensional numerical modeling of the river conducted by Ayers (Table 3 of data faxed from Scott Hogan to Art Glickman, January 31, 1997).

For river flows under about 20,000 ft^3/s, the GF2 and check structure result in a significant increase in the water surface at the screens compared to previous concepts tested without these structures. This could result in future changes in the screen length or invert elevation. However, for the tests reported herein, the length of the screen modeled was 1056 ft (length used in the previous model tests), including bypasses and screen area lost to structural members. The unobstructed screen area tested in the model was ~10,000 ft^2 prototype or ~10 percent more than the minimum required to meet criteria. Therefore, the final screen length may be reduced or the invert elevation raised.

Summary of Model Tests

The new screen layout was tested over a range of river conditions between 5,000 ft^3/s and 40,000 ft^3/s referenced to the north island river gauge (NIRG). Sweeping and approach velocities were measured using a 3-dimensional acoustic doppler velocity meter. Velocities were measured at the center of each screen bay on the new screen and at every fourth bay on the existing screen. At each location, sweeping and approach velocity was measured at a rate of 5 hertz as the velocity meter was slowly traversed from the water surface to the channel invert and back to the surface. The velocity meter was traversed through the water column at a constant speed using a traversing table.

Baffles were mounted vertically behind the entire screen. Prior to initial testing of the new screen layout, baffles were set based on the results from the previous screen layout to an opening of about 15 percent. Baffle settings were then adjusted during the testing of the new layout to achieve good uniformity of approach flow to the

screen. For all tests, intermediate fish bypass flows were set to 50 ft^3/s.

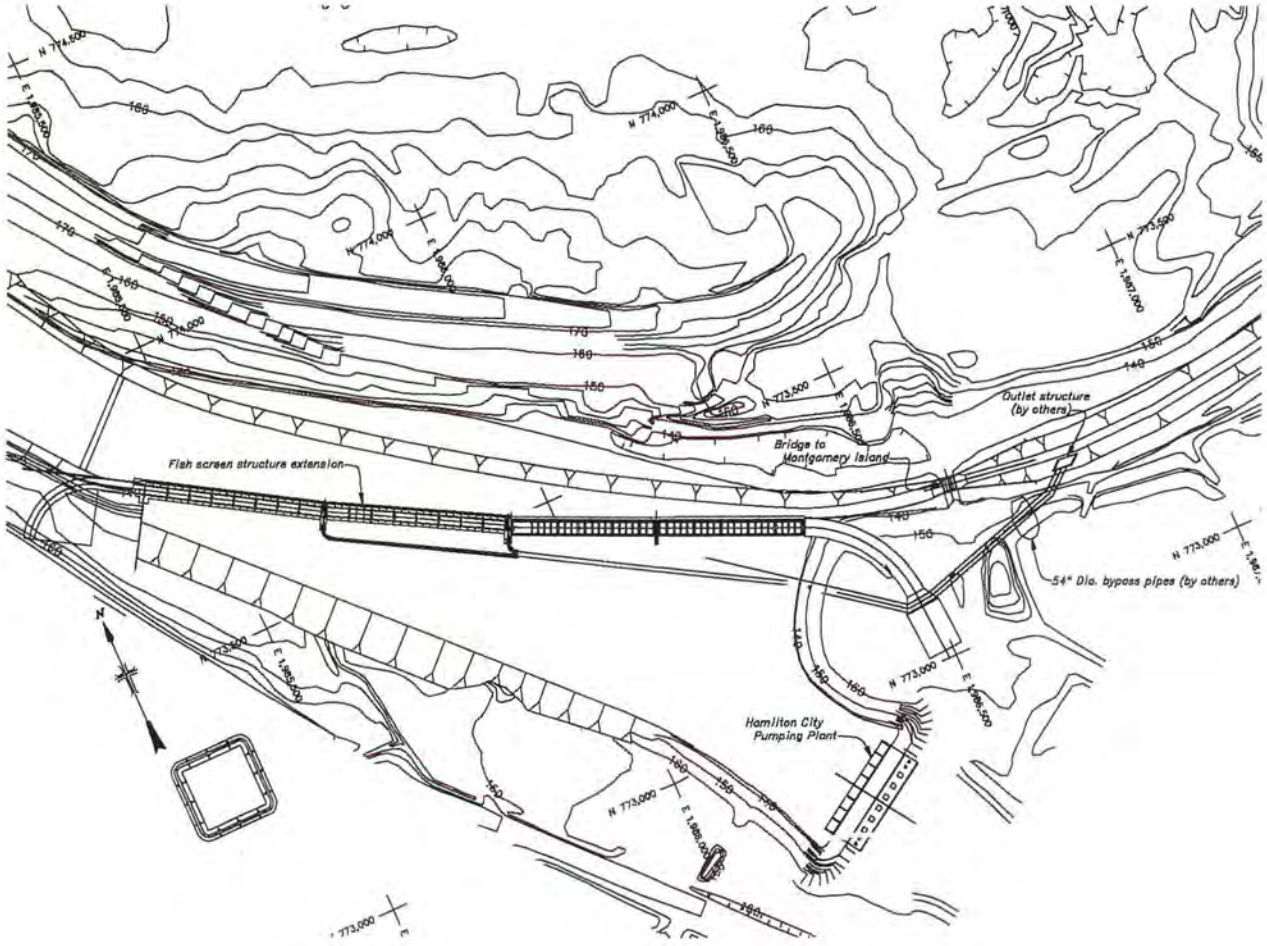

Figure 1 - Site plan for GCID fish screen.

Table 1. Hydraulic conditions at GCID for a GF2 with internal bypass system (Ayers, Jan. 1997).

Sacramento River Flow at North Island Gage (cfs)	GCID Intake Channel Diversion (cfs)	GCID Pumped Diversion (cfs)	GCID Internal Bypass Discharge (cfs)	Flow in GCID Bypass Channel (cfs)	Sacramento River Flow at South Island Gage (cfs)	WSEL at North Island Gage (ft)	WSEL at GCID Fish Screens (ft)	WSEL at South Island Gage (ft)
5000	1570	1000	150	420	4000	137.5	137.4	134.2
7000	3500	3000	150	350	4000	137.5	137.0	134.2
8000	3590	3000	150	440	5000	137.9	137.4	134.5
10000	3775	3000	150	625	7000	138.6	138.2	135.2
20000	4750	3000	150	1600	17000	141.1	140.9	137.9

Sacramento River Flow at North Island Gage (cfs)	Discharge at Check Structure (cfs)	Upstream WSEL at Check Structure (ft)	Downstream WSEL at Check Structure (ft)	Head Differential Between Fish Screens and S. Island Gage (ft)	Head Differential Between N. Island and S. Island Gages (ft)	GCID Intake Channel Velocity (fps)	Average Maximum Bypass Channel Velocity (fps)	Average Minimum Bypass Channel Velocity (ps)
5000	420	137.4	134.8	3.2	3.3	1.0	1.8	1.0
7000	350	137.0	134.6	2.8	3.3	2.3	1.5	1.5
8000	440	137.4	135.0	2.9	3.4	2.3	1.8	1.8
10000	625	138.2	135.8	3.0	3.4	2.2	2.3	2.2
20000	1600	140.8	139.0	3.0	3.2	2.1	3.7	3.5

Model Test Results

The high water surface on the screen (compared to previous tests for the no-GF option) created by the gradient facility in the river and the check structure in the lower oxbow resulted in a gradual reduction of sweeping velocities along the screen. An example data set for 7,000 ft^3/s river flow and 3,000 ft^3/s pumping flow is shown in Figure 2. Screen bays are labeled from downstream to upstream in increasing order. Sweeping velocity decreases from upstream to downstream along the screen, falling below 2.0 ft/s at about bay 45. To increase sweeping velocity, the approach channel in front of the screen structure was narrowed by moving the opposite bank guide wall closer to the screen. In the model, the opposite bank guide wall was extended into the channel by adding a toe berm with a 2:1 slope to elevation 141. The berm was started across from the upstream-most fish bypass (between screen bays 48 and 49) and extended downstream to the entrance of the open channel fish bypass. Above elevation 141 the previous bank was left in place. The toe berm starts tangent to the existing bank at its upstream end and gradually increases in width along its length. At the downstream end of the screen, the channel invert is constricted to 14 ft, the width of the open bypass channel, see figure 1.

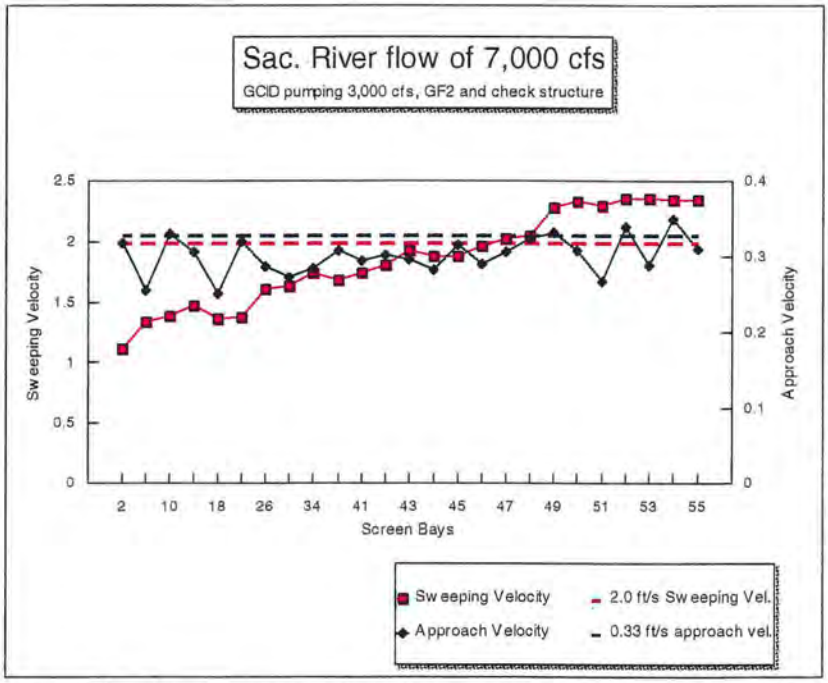

Figure 2. - Screen approach and sweeping velocity data for the screen layout shown in figure 1, water surface data given in Table 1 and the opposite bank guide wall alignment developed for the previous no-gradient-facility option.

Narrowing the approach channel increased flow sweeping velocity in front of the screen to about 2.0 ft/s or greater for NIRG flows of ≥7,000 ft^3/s. Sweeping and approach flow velocities measured 0.25 ft in front of the

screen are given in figures 3 through 6 for NIRG flows of 5,000 ft^3/s; 7,000 ft^3/s; 10,000 ft^3/s and 20,000 ft^3/s. The flow velocity data presented was measured for a fixed baffle position for all river flows tested. The data shows the fish screen structure tested can achieve good uniformity of approach velocity along the screen and high sweeping velocities for the normal conditions under which GCID diverts water.

Screen Bay DS-to-US	Sweeping Velocity ft/s	Approach Velocity ft/s
2	1.1872	0.0416
6	1.4	0.0768
10	1.2848	0.0936
14	1.1872	0.098
18	1.1188	0.1124
22	0.9924	0.1648
26	0.9844	0.1276
30	0.9544	0.1296
34	0.9052	0.1284
38	0.9552	0.11
41	0.8276	0.0972
42	0.9528	0.1308
43	0.9772	0.1092
44	0.9484	0.1292
45	0.9872	0.1372
46	0.97	0.126
47	0.9732	0.126
48	0.9852	0.1144
49	1.1116	0.1352
50	1.0648	0.1172
51	1.0408	0.1028
52	1.0668	0.1264
53	1.0664	0.1012
54	1.0444	0.1248
55	1.0988	0.1048

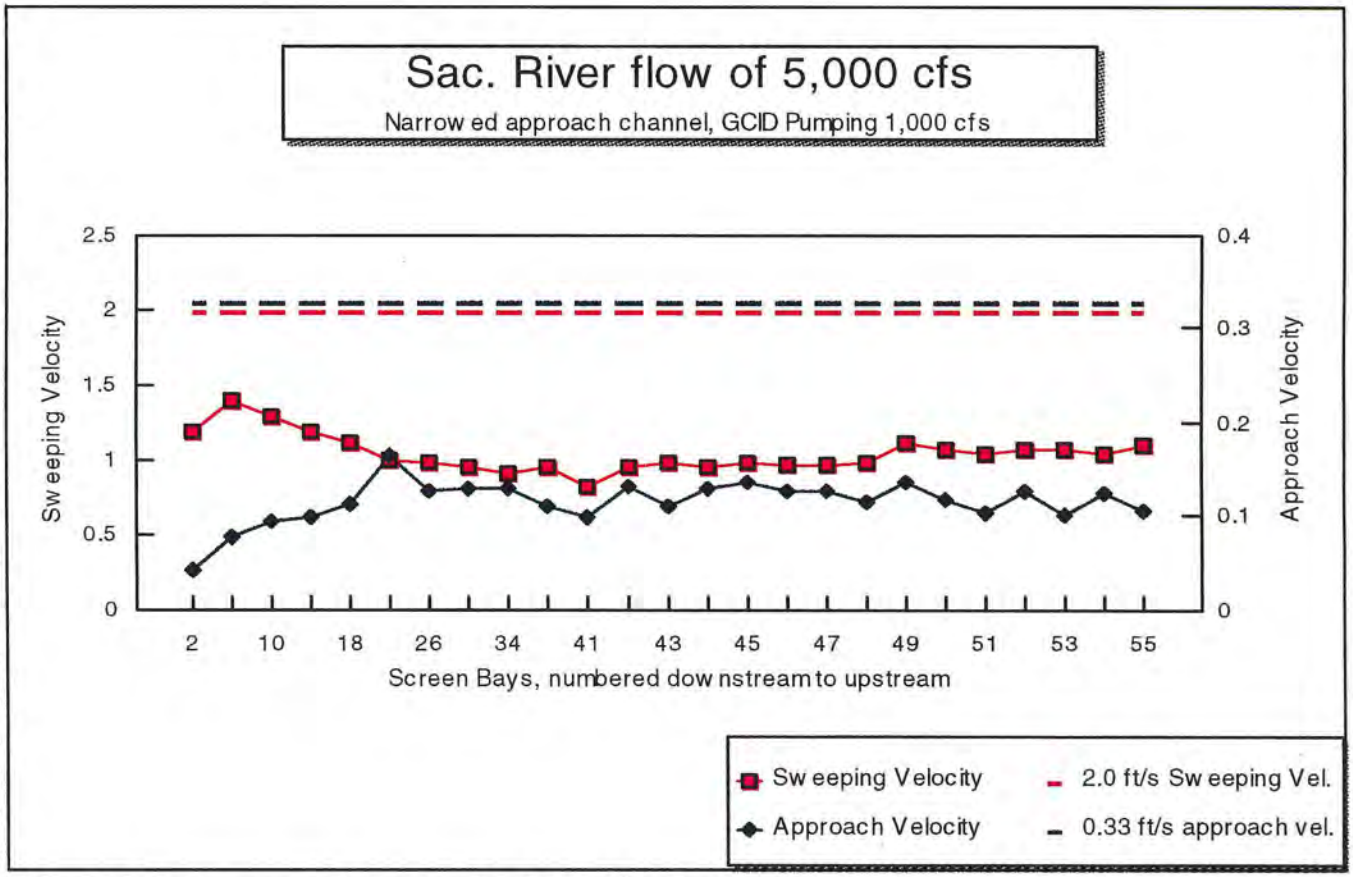

Figure 3 - Near screen velocity data for 5,000 ft^3/s river flow and 1,000 ft^3/s GCID diversion flow.

Screen Bay DS-to-US	Sweeping Velocity ft/s	Approach Velocity ft/s
2	1.8332	0.2844
6	1.9748	0.3096
10	1.9932	0.3008
14	2.1372	0.2896
18	2.098	0.3412
22	1.876	0.3668
26	1.848	0.3228
30	1.9416	0.3304
34	1.9244	0.3444
38	1.77	0.2916
41	1.8432	0.2908
42	1.9192	0.2996
43	1.878	0.2728
44	1.9716	0.306
45	2.1736	0.3624
46	2.0864	0.298
47	2.118	0.3108
48	2.2468	0.2892
49	2.416	0.3332
50	2.3696	0.2932
51	2.2664	0.2852
52	2.3212	0.3232
53	2.3712	0.2548
54	2.3248	0.312
55	2.3752	0.2732

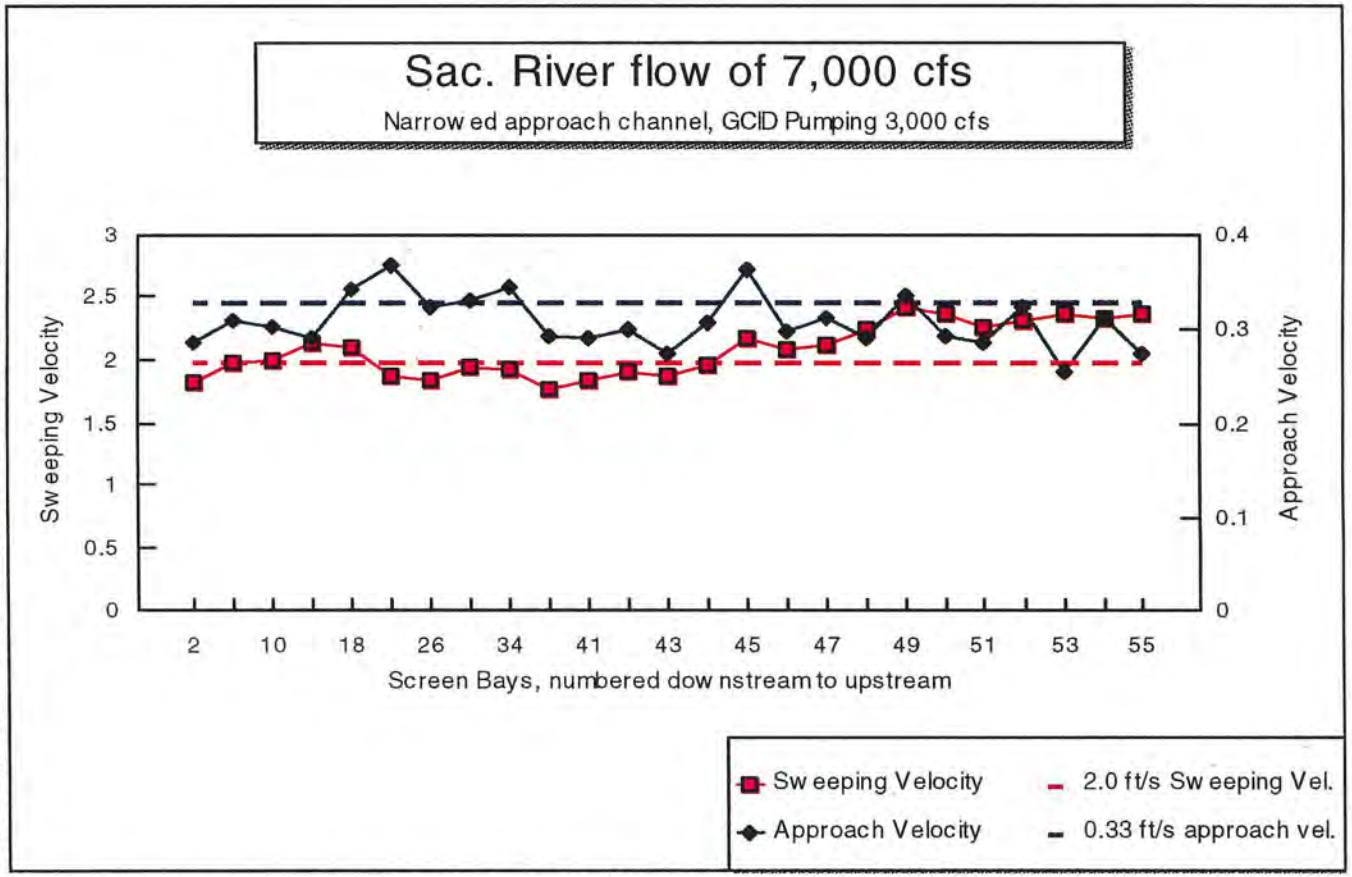

Figure 4 - Near screen velocity data for 7,000 ft^3/s river flow and 3,000 ft^3/s GCID diversion flow.

Screen Bay DS-to-US	Sweeping Velocity ft/s	Approach Velocity ft/s
2	2.2688	0.2632
6	2.38	0.2984
10	2.416	0.26
14	2.292	0.2648
18	2.1488	0.278
22	2.088	0.3464
26	1.9392	0.3192
30	1.8032	0.2776
34	1.9572	0.3068
38	1.886	0.2596
41	1.8072	0.2556
42	1.9268	0.29
43	1.956	0.2612
44	1.9632	0.2816
45	2.0332	0.326
46	2.0468	0.2764
47	2.0612	0.2916
48	2.188	0.2708
49	2.35	0.3112
50	2.284	0.266
51	2.2588	0.254
52	2.3104	0.3104
53	2.3568	0.2344
54	2.328	0.294
55	2.3592	0.2476

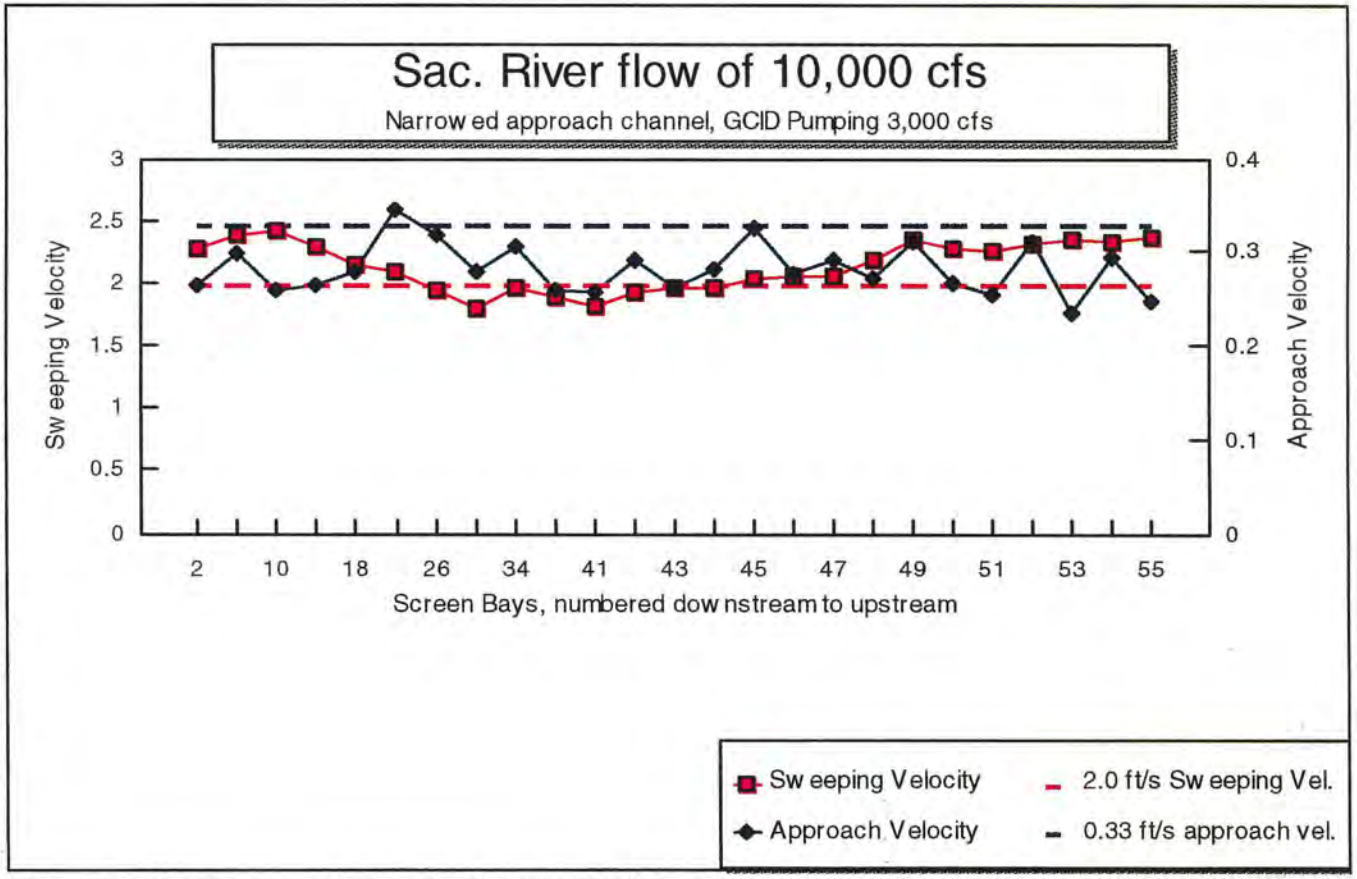

Figure 5 - Near screen velocity data for 10,000 ft^3/s river flow and 3,000 ft^3/s GCID diversion flow.

Screen Bay DS-to-US	Sweeping Velocity ft/s	Approach Velocity ft/s
2	2.5968	0.0552
6	3.3912	0.174
10	3.1532	0.2244
14	2.908	0.2184
18	2.6028	0.2364
22	2.4228	0.3176
26	2.3432	0.292
30	1.8392	0.2444
34	2.2344	0.2976
38	2.1984	0.2492
41	2.0652	0.2724
42	2.1192	0.2712
43	2.1404	0.26
44	1.818	0.2712
45	2.1548	0.3344
46	1.9128	0.2524
47	2.102	0.286
48	2.2728	0.2688
49	2.4716	0.3364
50	2.4448	0.2972
51	2.156	0.2336
52	2.4396	0.322
53	2.3668	0.2216
54	2.3432	0.2928
55	2.3836	0.258

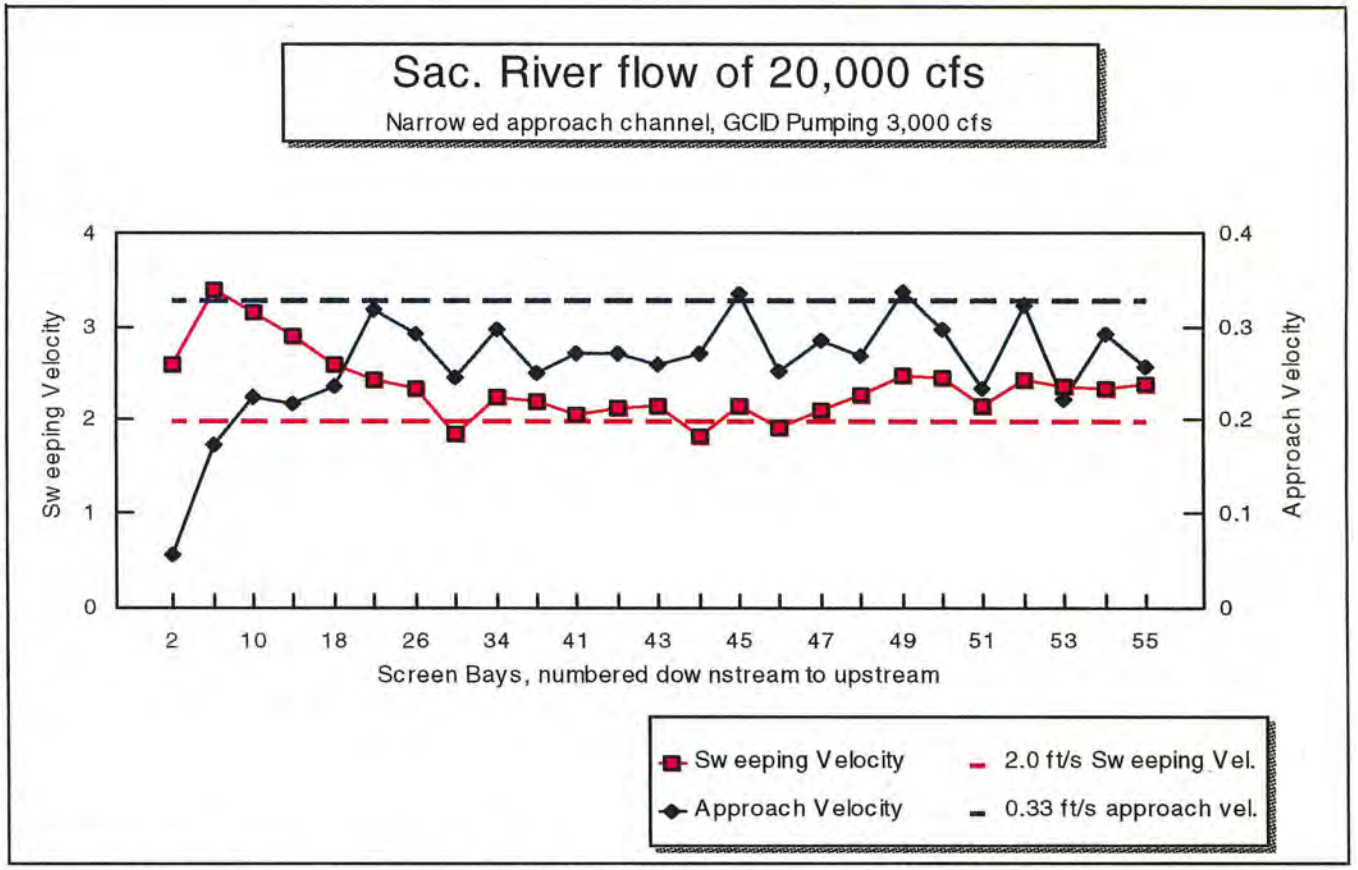

Figure 6 - Near screen velocity data for 20,000 ft^3/s river flow and 3,000 ft^3/s GCID diversion flow.

Tests of Baffle Location

Following testing of the new layout, several tests on the effect of baffle position were conducted. Baffles on the new screen were removed from behind the screen and mounted on the downstream side of the piers. Baffles on the existing screen structure were not changed as this would have required extensive modifications of the model baffles due to the shape and narrow spacing of the piers. Mounting the baffles vertically behind the screen (as previously tested) results in an average distance of 2.0 ft between the screen and the baffles. This area is open along the entire length of the screen face. The uncontrolled flow area (2.0 ft* water depth) is about one third that of the open area of the baffles per screen bay (0.15* distance between piers). Moving the baffles to the downstream side of the piers resulted in an average distance between the screen and the front nose of the piers of 5.9 ft and a flow area approximately equal to that of the open area through the baffles.

Model tests were conducted for NIGR flows of 7,000 ft^3/s, 10,000 ft^3/s, and 20,000 ft^3/s. For each flow condition, baffles on the new screen structure were adjusted to achieve nearly uniform screen approach flow velocity. However, establishing acceptable uniformity of approach flow to the screen with the baffles placed behind the piers was difficult. The large uncontrolled flow area between the screens and the pier noses resulted in poor control of flow through the screens. After several iterations of adjusting baffles, the best approach flow conditions were achieved by using a range of baffle settings between 0 and 15 percent open area, figure 7. Near screen velocity profiles for each flow tested with the baffles behind the piers are given in figures 8, 9, and 10. Placing the baffles behind the piers resulted in substantially less control over the screen approach velocities than found with the baffles mounted behind the screens. Based on the limited testing conducted, the uncontrolled area between the screen and the baffles or pier noses should not exceed about 15 percent of the screen open area measured between piers.

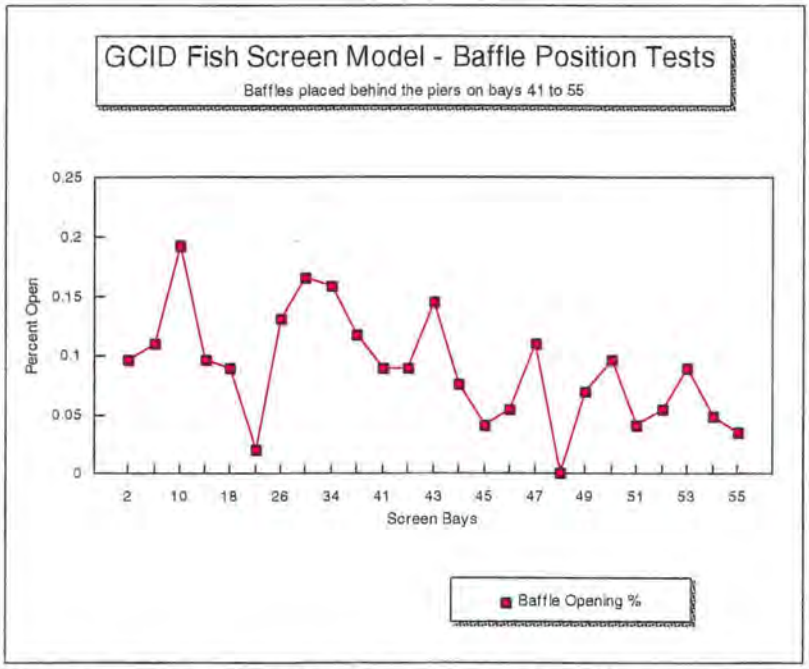

Figure 7 - Variability of baffle settings with baffles positioned behind the piers on the new screen structure.

Screen Bay DS-to-US	Sweeping Velocity ft/s	Approach Velocity ft/s
2	1.8436	0.3324
6	2.0688	0.3748
10	2.2732	0.3432
14	2.3048	0.3592
18	2.2964	0.3516
22	1.9692	0.2852
26	2.0176	0.3824
30	2.1156	0.3788
34	2.1744	0.3996
38	2.2184	0.296
41	2.0336	0.3
42	2.1844	0.3348
43	2.246	0.3532
44	2.2704	0.2988
45	2.3792	0.3204
46	2.3636	0.2976
47	2.3772	0.3552
48	2.366	0.358
49	2.4744	0.3252
50	2.6136	0.3316
51	2.5044	0.306
52	2.4592	0.3016
53	2.4612	0.3508
54	2.3652	0.296
55	2.534	0.3992

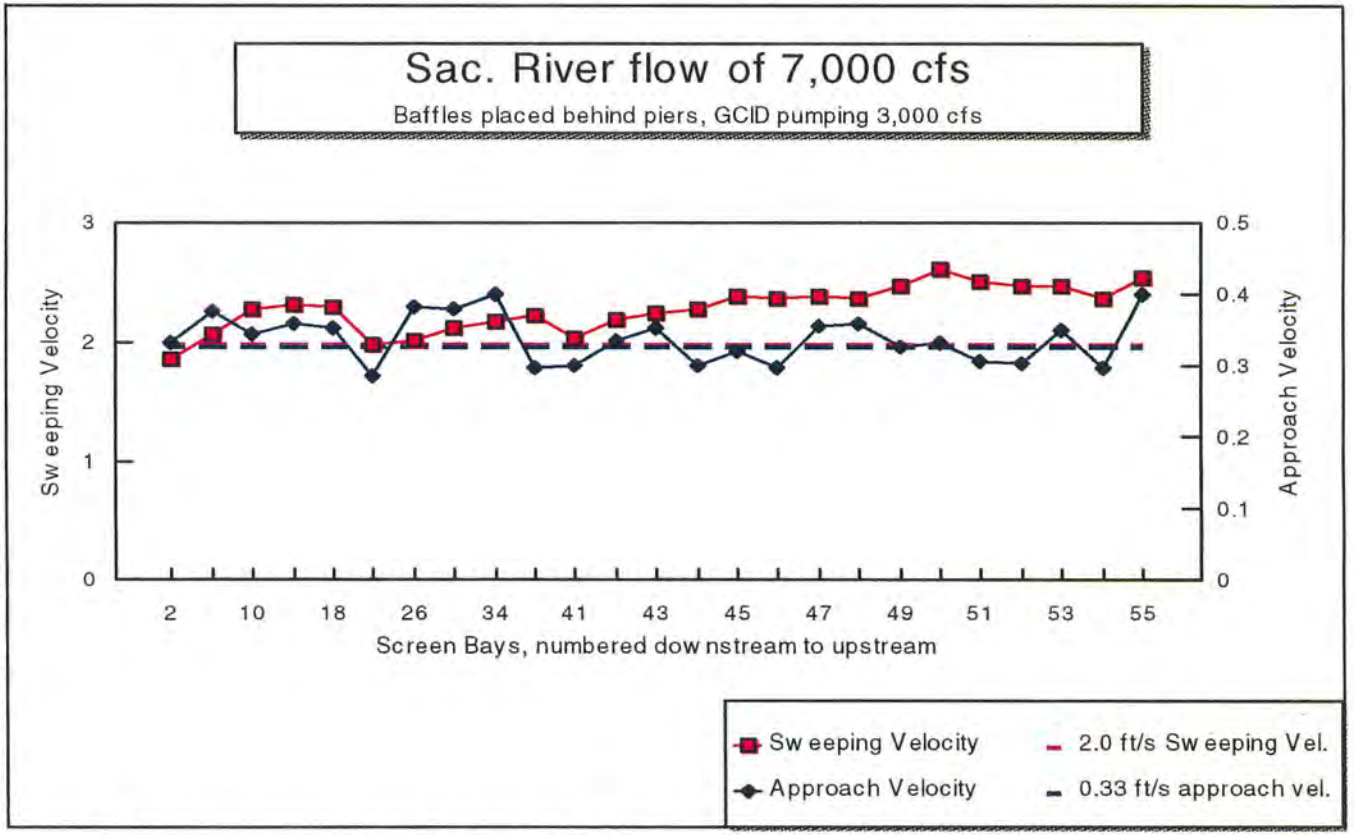

Figure 8 - Near screen velocity data for 7,000 ft^3/s river flow and 3,000 ft^3/s GCID diversion flow. Baffles placed behind the piers on the new screen.

Screen Bay DS-to-US	Sweeping Velocity ft/s	Approach Velocity ft/s
2	2.414	0.334
6	2.594	0.3036
10	2.6244	0.2972
14	2.636	0.312
18	2.3868	0.3404
22	2.2952	0.3852
26	2.1816	0.3224
30	2.2496	0.3252
34	2.2208	0.332
38	2.2412	0.2536
41	2.0244	0.2656
42	2.178	0.2828
43	2.166	0.3008
44	2.2276	0.2692
45	2.274	0.29
46	2.2216	0.2752
47	2.2792	0.2616
48	2.2696	0.3016
49	2.4468	0.2804
50	2.422	0.3148
51	2.4292	0.4016
52	2.448	0.3056
53	2.4208	0.3264
54	2.4308	0.278
55	2.4328	0.316

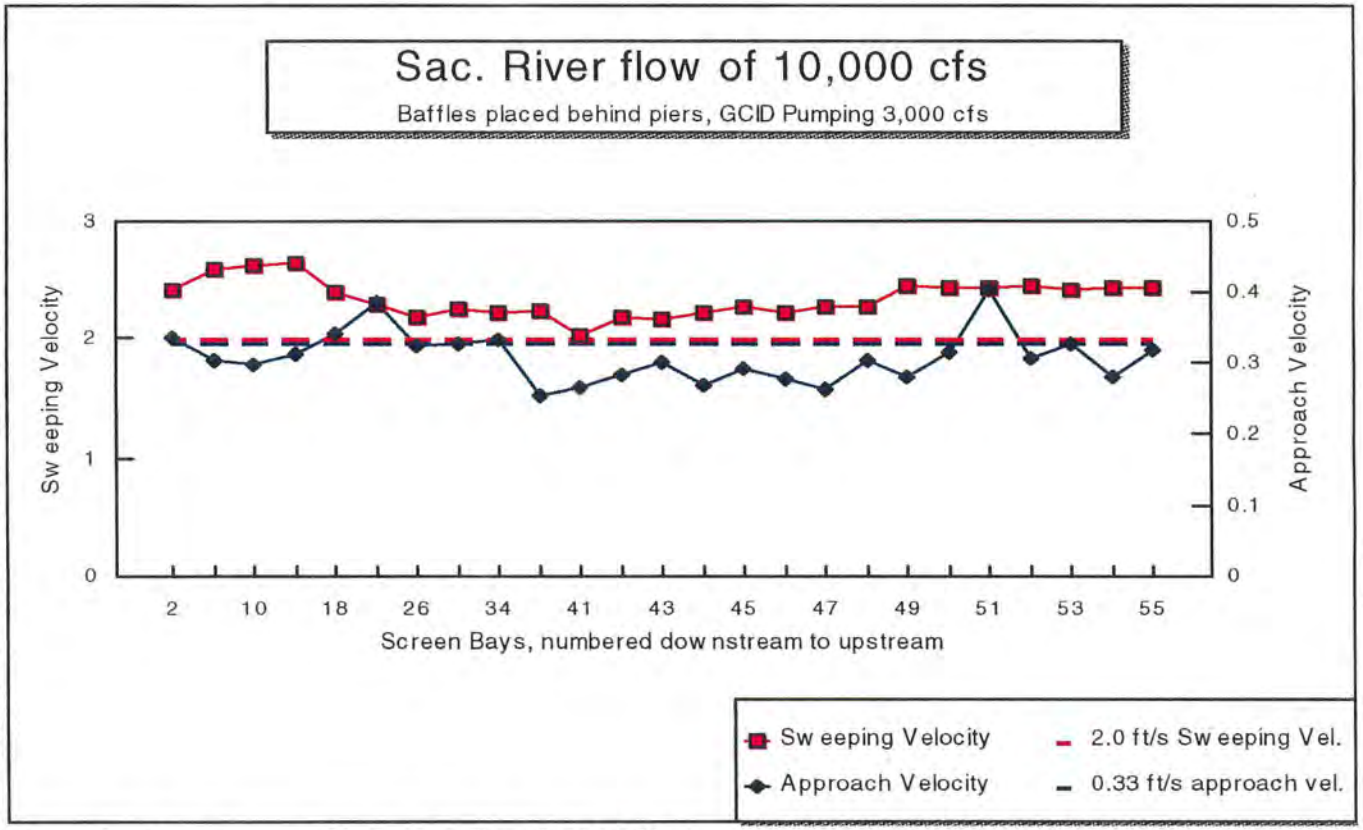

Figure 9 - Near screen velocity data for 10,000 ft^3/s river flow and 3,000 ft^3/s GCID diversion flow. Baffles placed behind the piers on the new screen.

Screen Bay DS-to-US	Sweeping Velocity ft/s	Approach Velocity ft/s
2	3.6572	0.2196
6	3.5236	0.242
10	3.3524	0.2528
14	3.1636	0.2616
18	2.8084	0.2728
22	2.644	0.3532
26	2.5448	0.3068
30	2.346	0.3276
34	2.3872	0.3104
38	2.4048	0.2464
41	2.228	0.256
42	2.4056	0.2876
43	2.3824	0.3036
44	2.3896	0.256
45	2.3788	0.2872
46	2.3548	0.28
47	2.3	0.2752
48	2.272	0.2972
49	2.3288	0.2768
50	2.5324	0.3192
51	2.4616	0.36
52	2.4112	0.296
53	2.3524	0.3044
54	2.2916	0.25
55	2.414	0.334

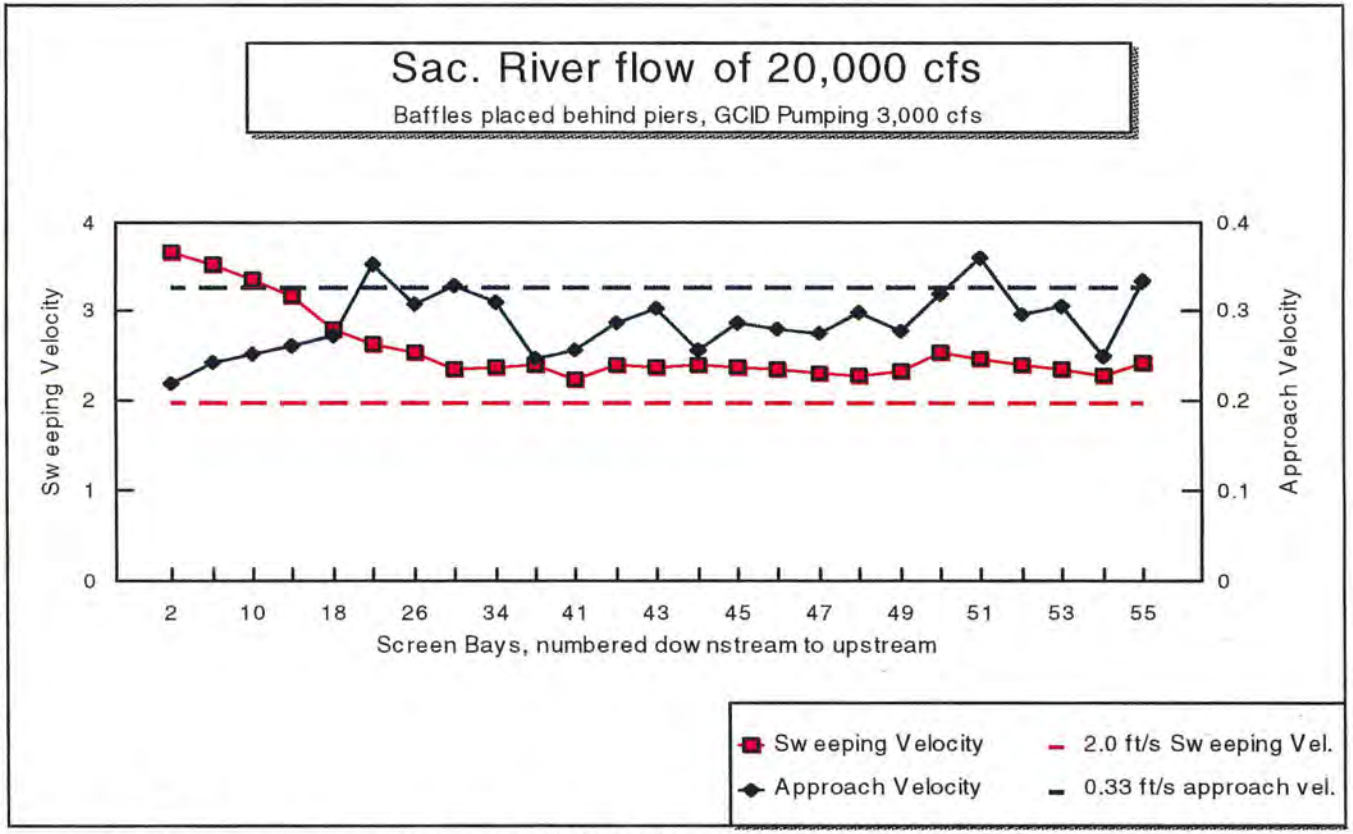

Figure 10 - Near screen velocity data for 20,000 ft^3/s river flow and 3,000 ft^3/s GCID diversion flow. Baffles placed behind the piers on the new screen.

Fish Bypass Model

A 1:5 scale model of an internal fish bypass was constructed in the Water Resources Research Laboratory (WRRL), figure 11. The model simulated 10 ft of flow width passing in front of the bypass, the bypass entrance, trashrack, adjustable weir, and transition to the bypass pipe. Flow through the adjacent fish screen was not modeled. A solid boundary was used in place of screen. The model was constructed to evaluate:

- The hydraulic performance of an adjustable slope "/\" shaped weir, including energy loss and weir discharge coefficient, figure 12.
- The hydraulic performance of an adjustable vertical weir with fixed approach and downstream ramps, figure 13.
- The hydraulic performance of the bell mouth bypass entrance.
- The local influence of the bypass flow on screen approach flow conditions upstream and downstream of the bypass.

The objective of a fish bypass is to entrain fish that are moving downstream in close proximity to the screen face. These fish are considered at risk of being impinged on the fish screen. After entering the bypass, fish are carried downstream through a pipe around the screen and check structure. Fish are reintroduced to the lower oxbow channel just downstream of the open channel bypass check structure. The bell mouth entrance to the bypass is designed to provide a gradual change in flow velocity such that fish close to the bypass are less likely to avoid the entrance. The adjustable weir in the bypass allows bypass flow to be regulated to maintain an entrance velocity close to that of the screen sweeping velocity. For each weir design, flow conditions are being evaluated surrounding the bypass entrance and within the weir and transition sections. Testing is complete for the adjustable ramp weir. Testing of the vertical weir design will start in May following feedback on the design from resource agencies.

Adjustable Ramp Weir Model Results

Flow calibration tests were conducted for the adjustable ramp weir for a range of weir heights and flows. Flow through the bypass was measured as a function of head on the weir and weir crest elevation. The results of these tests are given in figures 14 and 15. Discharge over the weir can be calculated from the coefficient of discharge data by the equation;

$$Q = C_d L \Delta H^{1.5}$$

where; Q = discharge
L = weir crest length
C_d = coefficient of discharge
ΔH = head on the weir

The performance of the bypass design was evaluated by collecting velocity data and injecting dye for flow visualization. Flow velocity was measured in front of the bypass entrance and in the bypass throat upstream of the

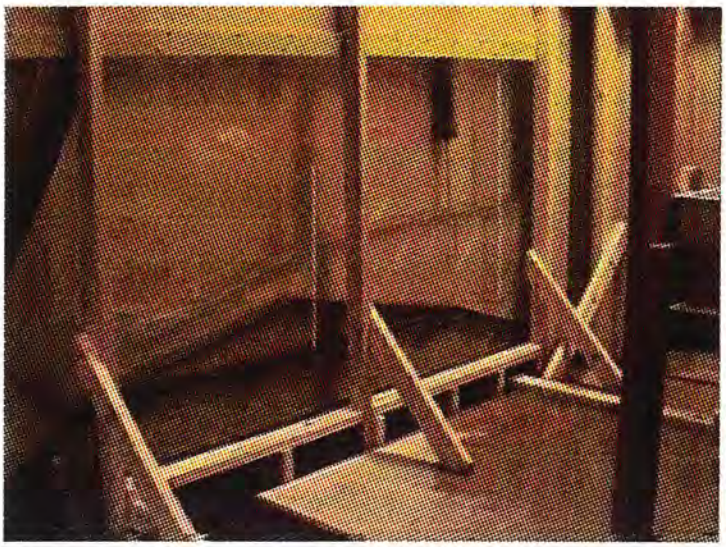

Figure 11 - Side view of the adjustable ramp weir fish bypass model.

measured with an acoustic doppler velocity meter. The model was tested for river water surface elevations corresponding to 7,000 ft^3/s (figures 18 to 22), 10,000 ft^3/s (figures 23 to 28), and 20,000 ft^3/s (figures 29 to 34). For each test, sweeping velocity upstream of the bypass was set at a reference velocity of 2 ft/s and the weir was adjusted to provide 50 ft^3/s flow through the bypass. Velocity data for each test is given as 2-dimensional velocity vector plots. X-Y velocity component vectors are given on plan views of the bypass entrance referenced to a distance above the invert. Velocities measured in the bypass throat are given as X-Z velocity vector components and are shown on an elevation view of the bypass structure. The data shows entrainment velocity profiles are fairly consistent over the range of weir operation. Flow velocity into the bypass is typically highest near the surface and decreases with depth. Velocities measured 2 ft above the invert (location n, figure 17) averaged about 0.75 percent of near surface velocity for all conditions tested. Dye tests and velocity measurements revealed flow is entrained into the bypass for a distance out from the screen face of about 2 ft, indicating a smooth branching of flow into the bypass and a good match of sweeping and bypass entrance velocities. Velocity vectors measured 2.5 ft in front of the bypass entrances show little effect of bypass operation. Flow entering the bypass does increase the angle at which flow attacks the screen surface to either side of the bypass entrance. This effect is seen in the velocity vectors measured at location K in the model. This effect was further studied by measuring the approach and sweeping velocity components traversing from upstream to downstream across a bypass entrance. Data was collected in the bypass model and in the screen model where flow through the screen was modeled. Figure 35 shows a velocity traverse measured in the bypass model along the plane of the screen face at mid-depth. The bell mouth of the bypass extends about 2.1 ft either side of the bypass centerline. The data shows flow turning into the bypass sharply increases the angle of attack to the plane of the screen for a distance of about 4 ft either side of the bypass centerline. Thus, screen adjacent to the bypass (within ±4 ft of the bypass centerline) would experience elevated approach velocities compared to the average approach velocity on the screen. These data were confirmed by the results of similar tests conducted on the 1:16 scale fish screen model, figures 36 to 38. The data shows this effect to a lesser degree extends about 20 ft downstream of the bypass. Similarly, sweeping velocity (velocity component parallel to the screen) is also affected, but in the opposite direction. The sweeping velocity component falls as flow turns into the bypass and then gradually recovers about 20 ft downstream of the bypass.

The adjustable ramp weir design provided good hydraulic conditions both upstream and downstream of the weir. Upstream of the weir, flow accelerated smoothly to the weir crest. Dye and confetti tests revealed no eddies or stagnation zones within the flow approaching the weir. For normal operation (proper weir settings), flow passes through critical near the weir crest and accelerates rapidly on the downstream weir slope forming a weak hydraulic jump at the interface with the tailwater. Flow then moves smoothly into the bypass pipe. The weak hydraulic jump does not appear to offer an area for fish to hold. Buoyant confetti added to the flow passed through this zone with only minor delay. Flow stays attached to the downstream weir surface for all flow conditions. By remaining attached to the downstream weir slope, the flow develops a short zone of sub-atmospheric pressure immediately downstream of the weir crest. This low pressure zone provides a lift force on the downstream ramp

which will require consideration during design to ensure stability during operation. Pressures on the downstream ramp were not measured in the model during this phase of the study. However, these data could be measured if the adjustable ramp weir concept is pursued further.

Major Conclusions for this Phase of Modeling

The results from this phase of the model studies for the GCID fish screen design support the following design assumptions:

- The revised layout of the screen with three internal fish bypasses, a gradient facility, and check structure providing water surfaces as given in Table 1 can meet approach and sweeping velocity criteria for the range of river flows between 7,000 ft^3/s and 20,000 ft^3/s provided the channel in front of the screen structure is narrowed by moving the opposite bank guide wall alignment to the position shown on figure 1.
- The area of the screen can likely be reduced by about 5 percent due to the increase in water surface elevation resulting from the gradient facility and check structure.
- The bell mouth entrance to the internal fish bypasses in combination with an adjustable weir provides a low velocity gradient entrance to the internal fish bypasses.
- Total bypass width measured from the upstream interface with the screen to the downstream interface with the screen should be at least 8 ft to avoid elevated levels of approach velocity adjacent to the bypass.
- The adjustable ramp weir provides good hydraulic conditions for moving fish into and through the bypass.
- The adjustable ramp weir concept would likely require a cable in the bypass flow upstream of the weir crest to adjust the weir.
- The weir design may be difficult to construct due to the weir length and wall clearances. Fine sediment may deposit under the raised weir requiring a method to flush material from beneath the weir.

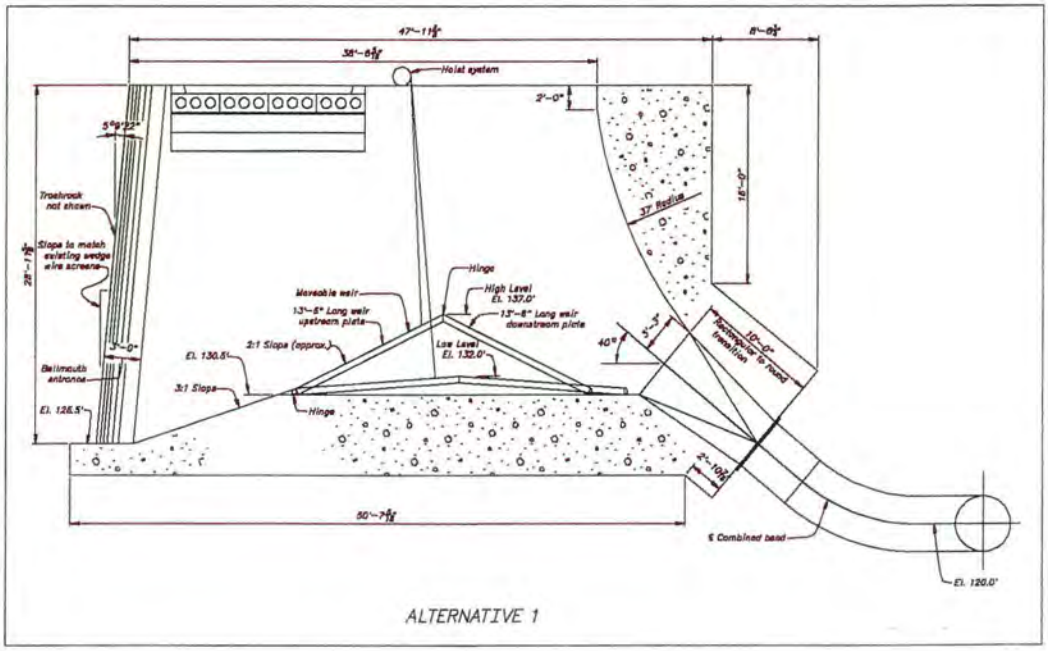

Figure 12 - Elevation view of adjustable height ramped weir concept for fish bypass.

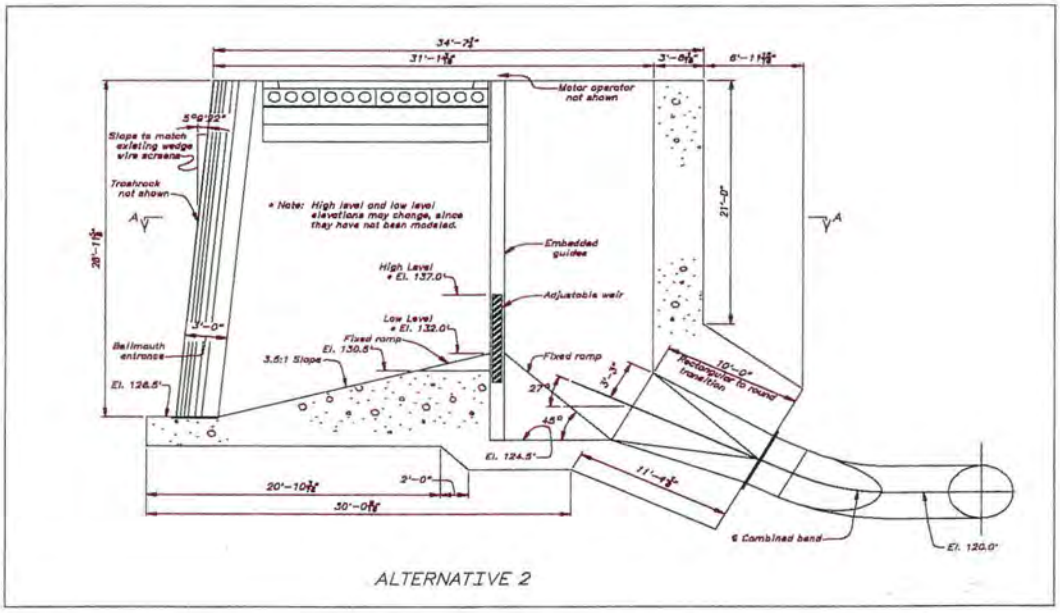

Figure 13 - Elevation view of adjustable vertical weir concept for fish bypass.

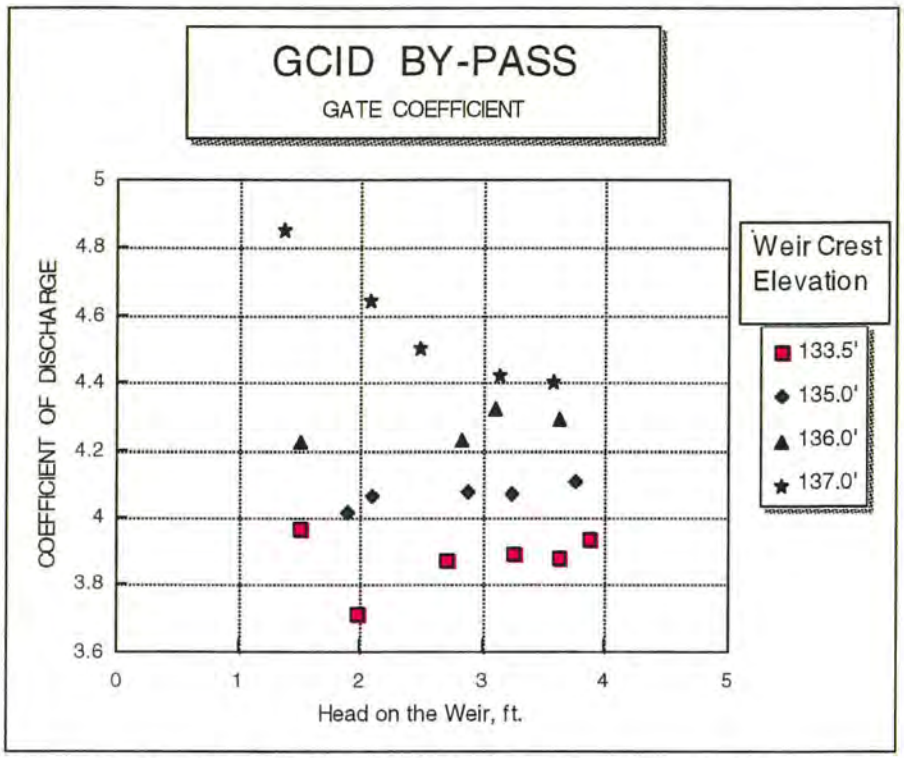

Figure 14 - Weir coefficient of discharge (Cd) versus Head for different weir crest elevations.

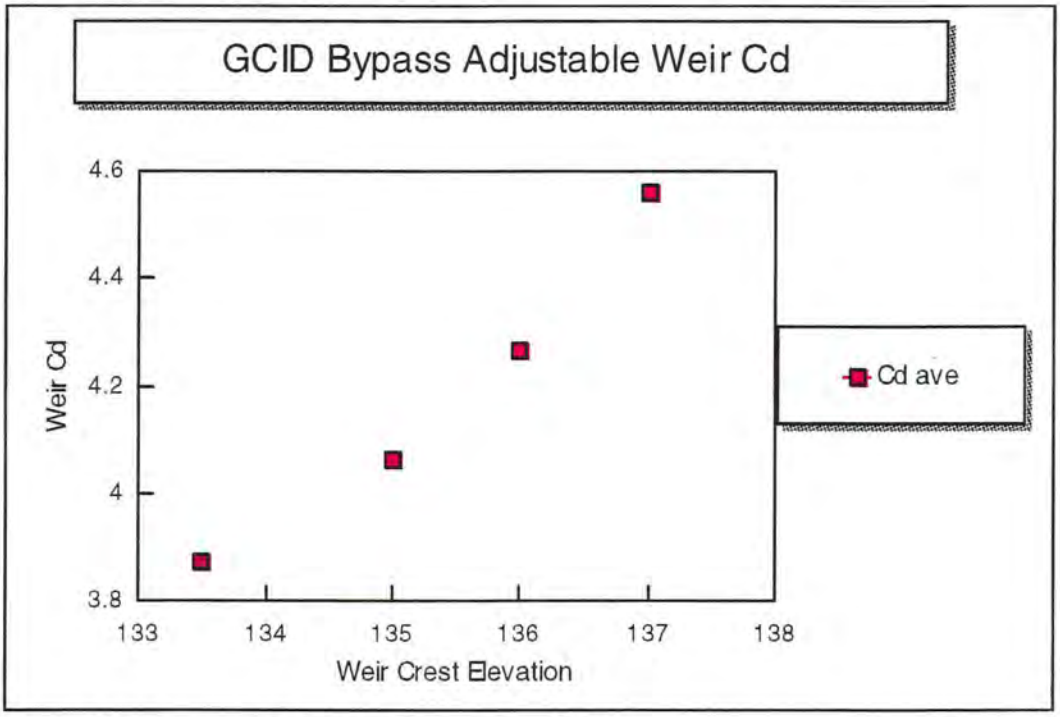

Figure 15 - Average Cd versus weir crest elevation.

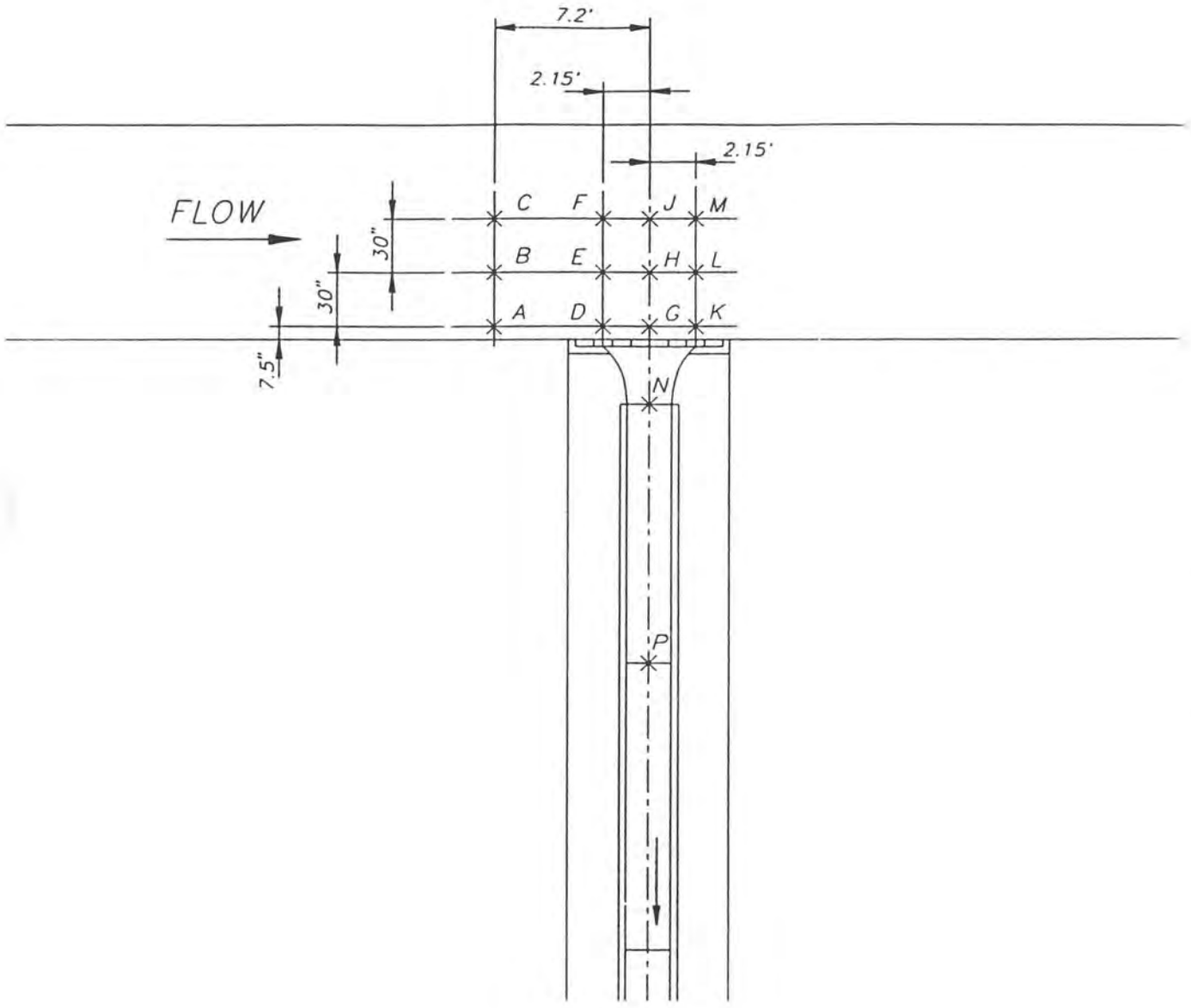

Figure 16 - Plan view of velocity measurement locations for the internal fish bypass.

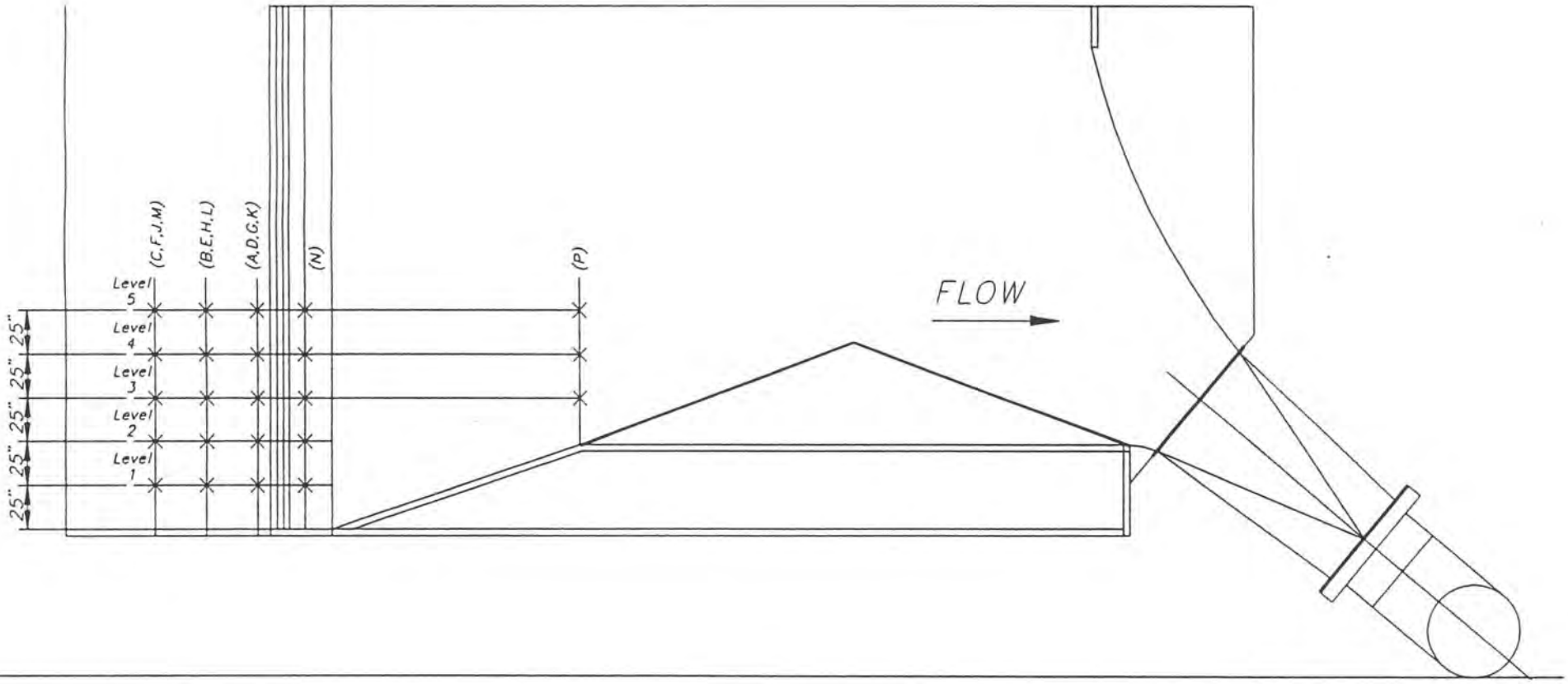

Figure 17 - Elevation view of velocity measurement locations for the internal fish bypass.

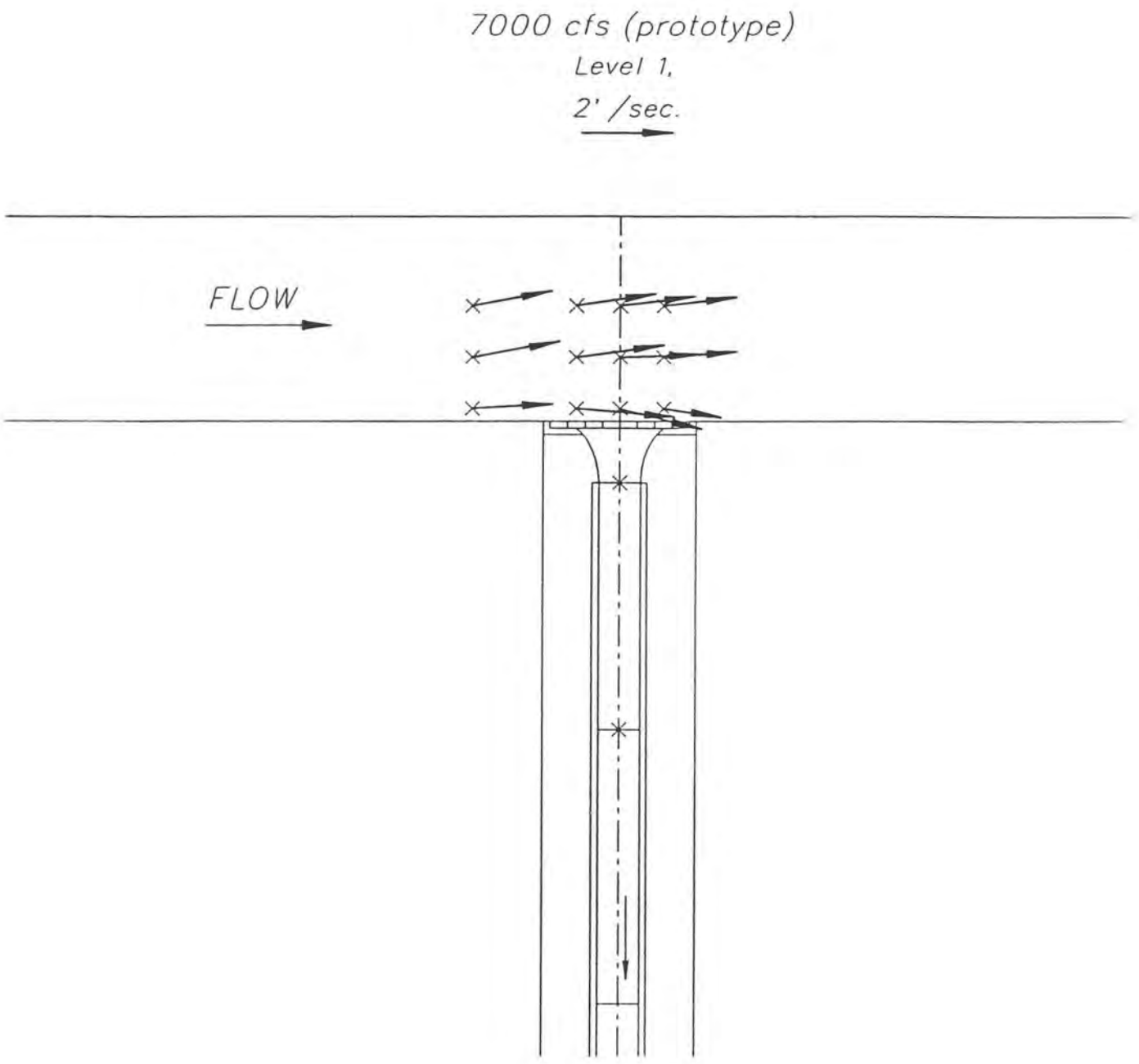

Figure 18 - Bypass entrance velocity vectors in X-Y plane measured 2.1 ft above the invert for 7,000 ft^3/s flow NIRG.

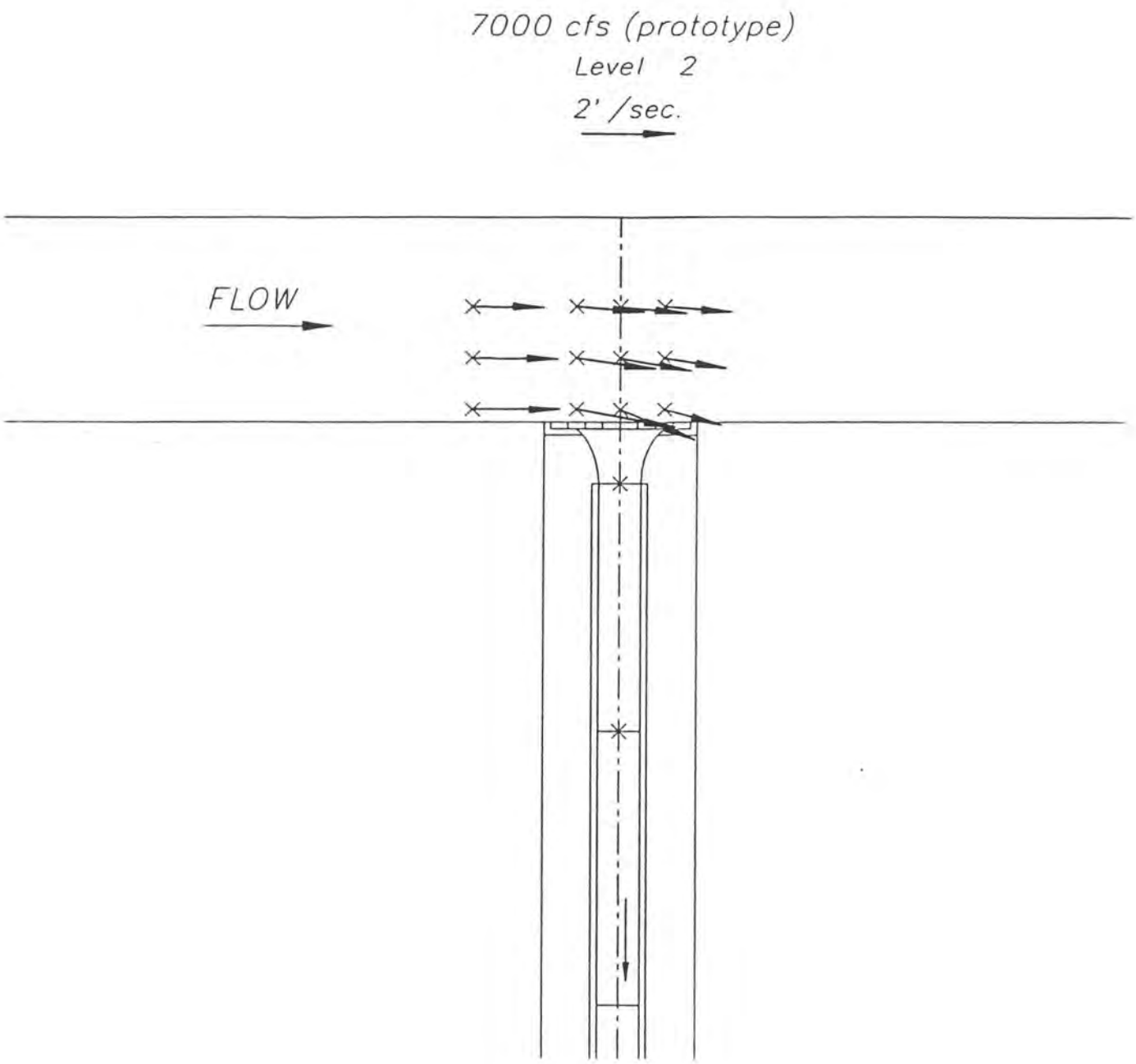

Figure 19 - Bypass entrance velocity vectors in X-Y plane measured 4.2 ft above invert for 7,000 ft^3/s flow NIRG.

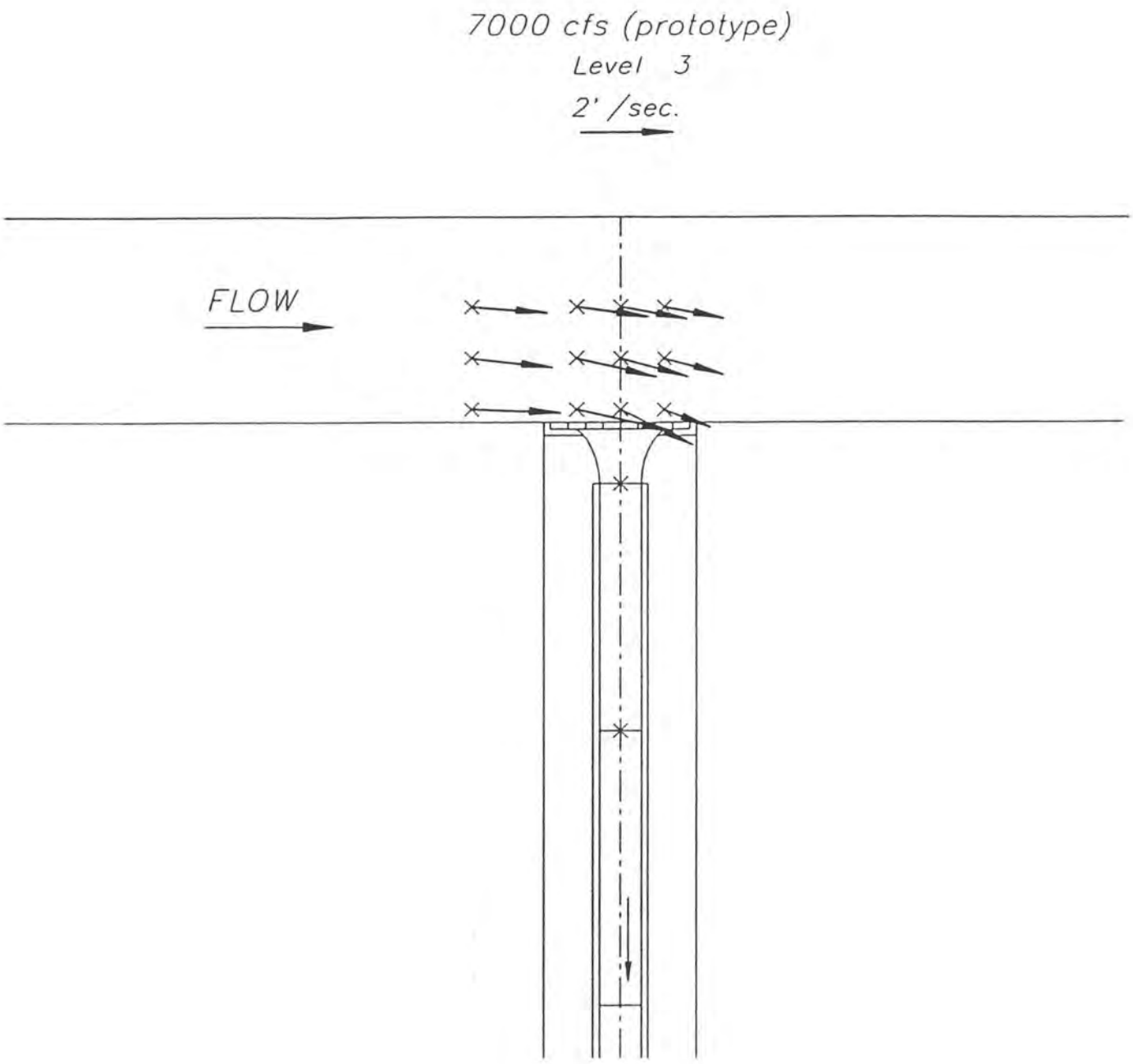

Figure 20 - Bypass entrance velocity vectors in X-Y plane measured 6.3 ft above invert for 7,000 ft^3/s flow NIRG.

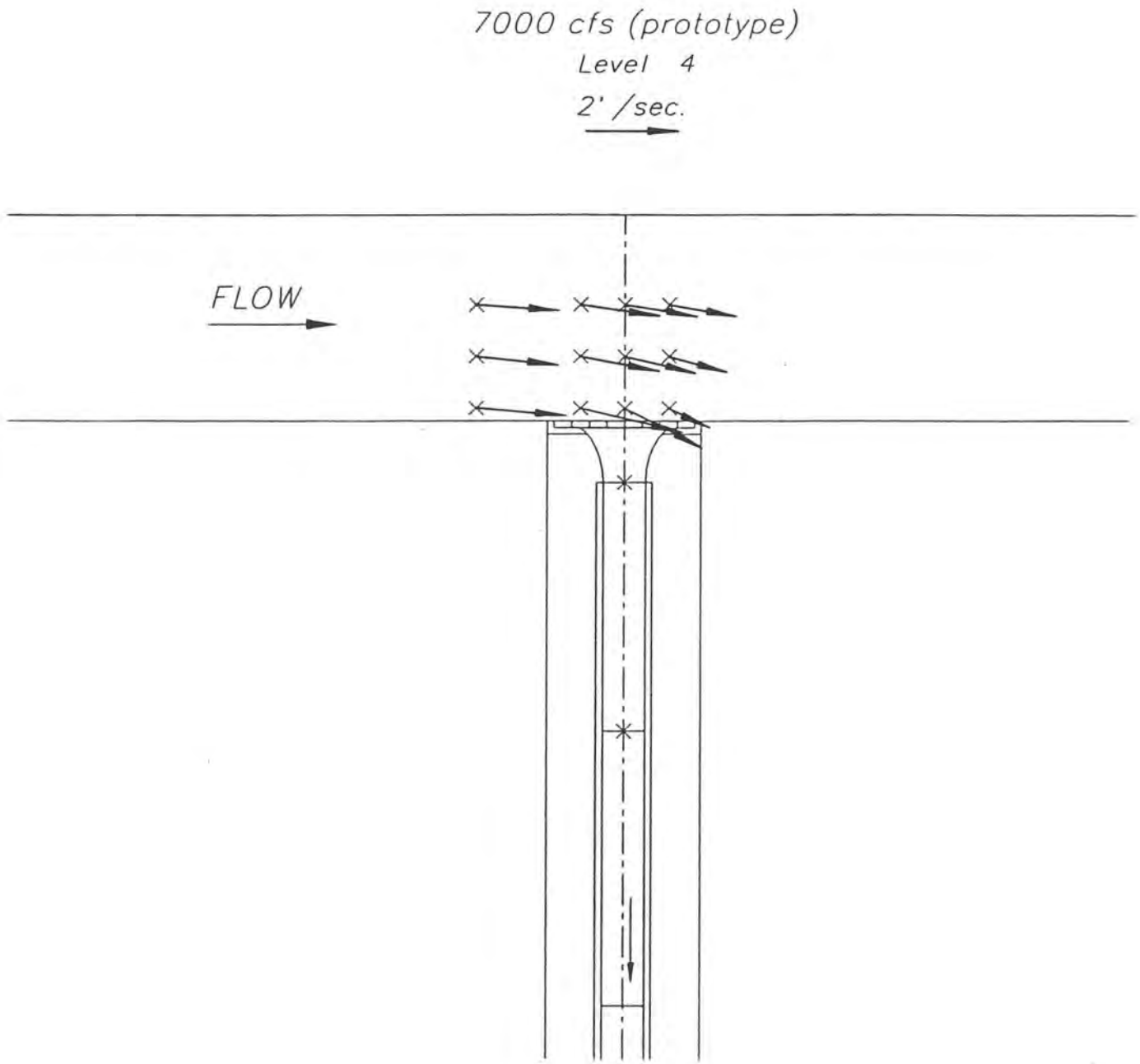

Figure 21 - Bypass entrance velocity vectors in X-Y plane measured 8.4 ft above invert for 7,000 ft^3/s flow NIRG.

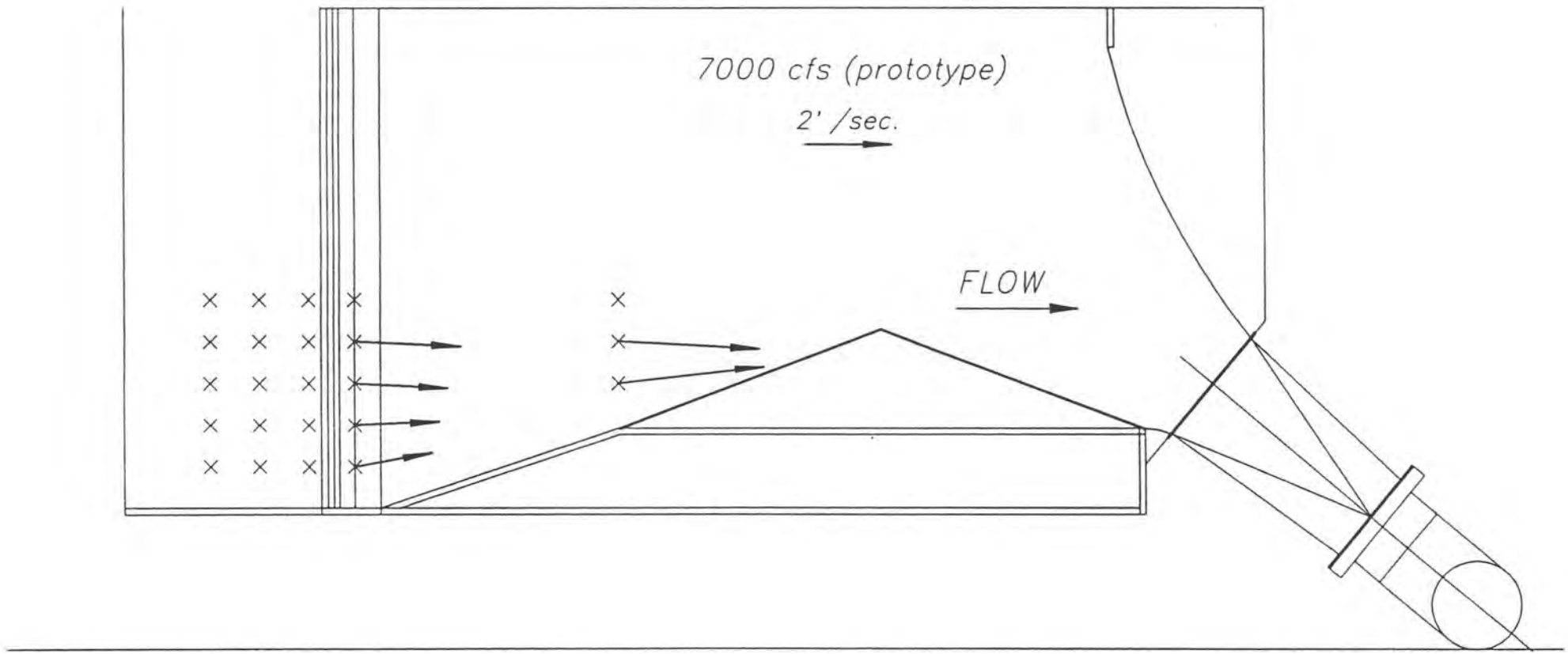

Figure 22 - Velocity vectors in X-Z plane measured in the bypass throat for 7,000 ft^3/s flow NIRG.

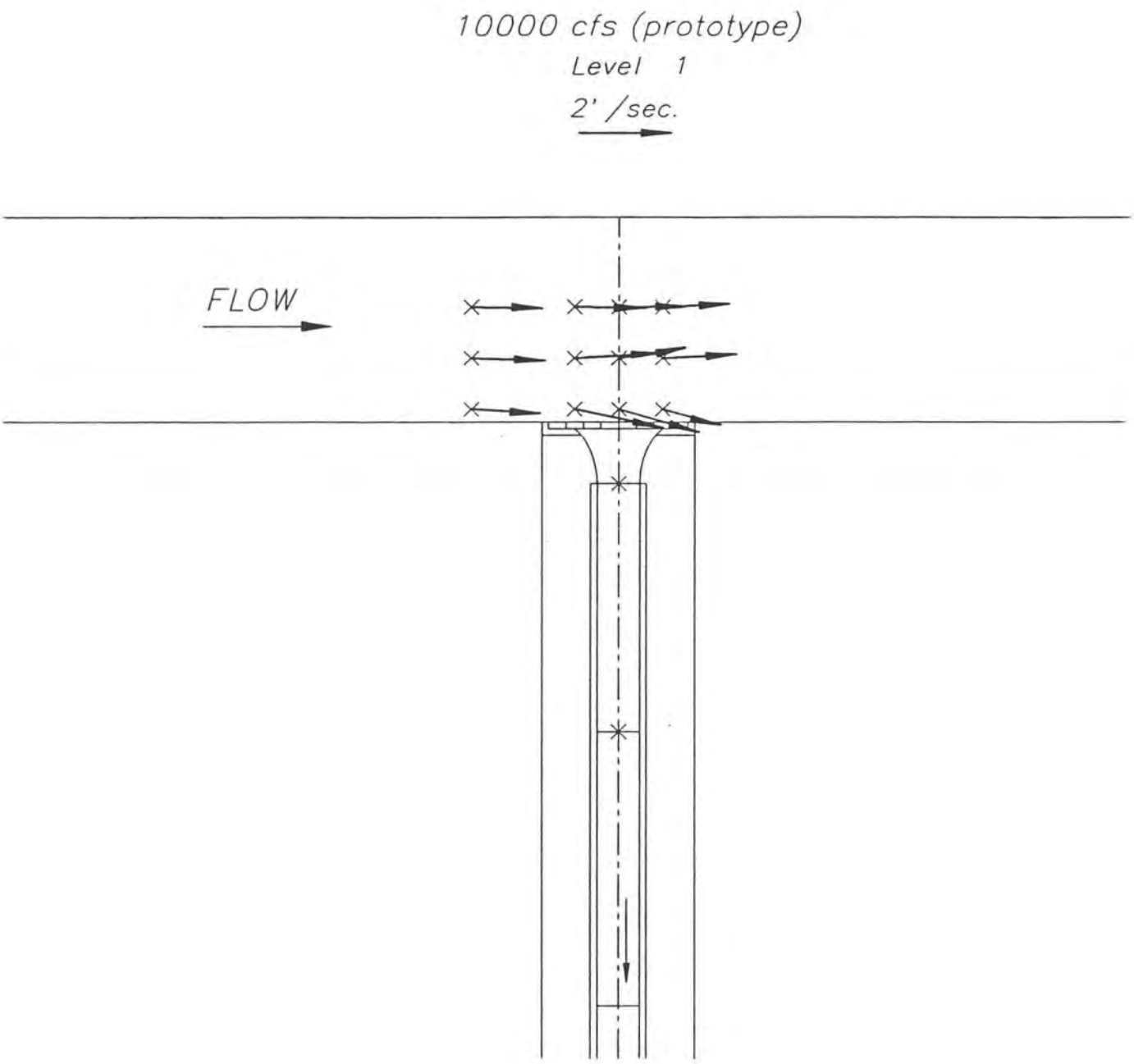

Figure 23 - Bypass entrance velocity vectors in X-Y plane measured 2.1 ft above the invert for 10,000 ft^3/s flow NIRG.

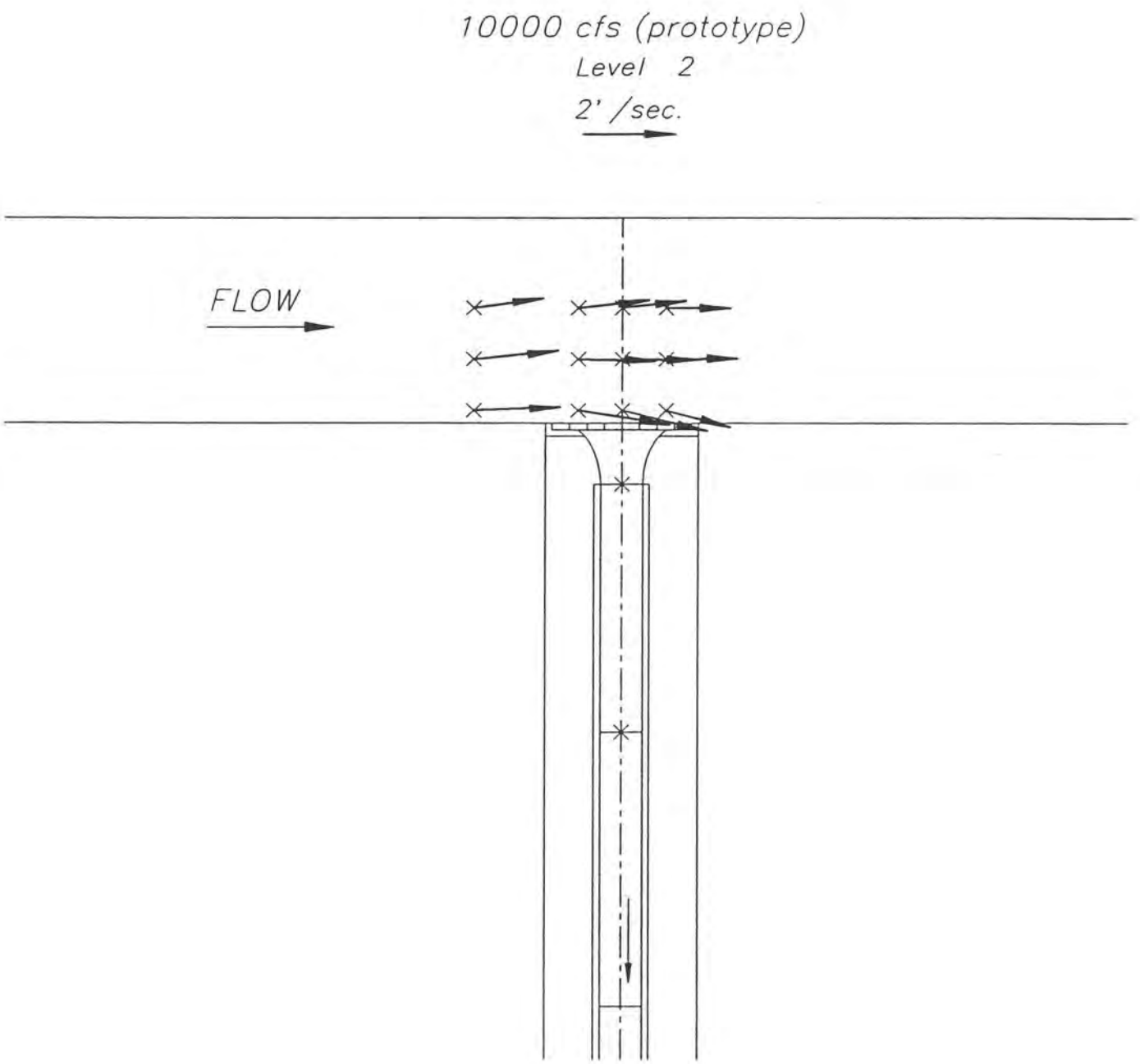

Figure 24 - Bypass entrance velocity vectors in X-Y plane measured 4.2 ft above the invert for 10,000 ft^3/s flow NIRG.

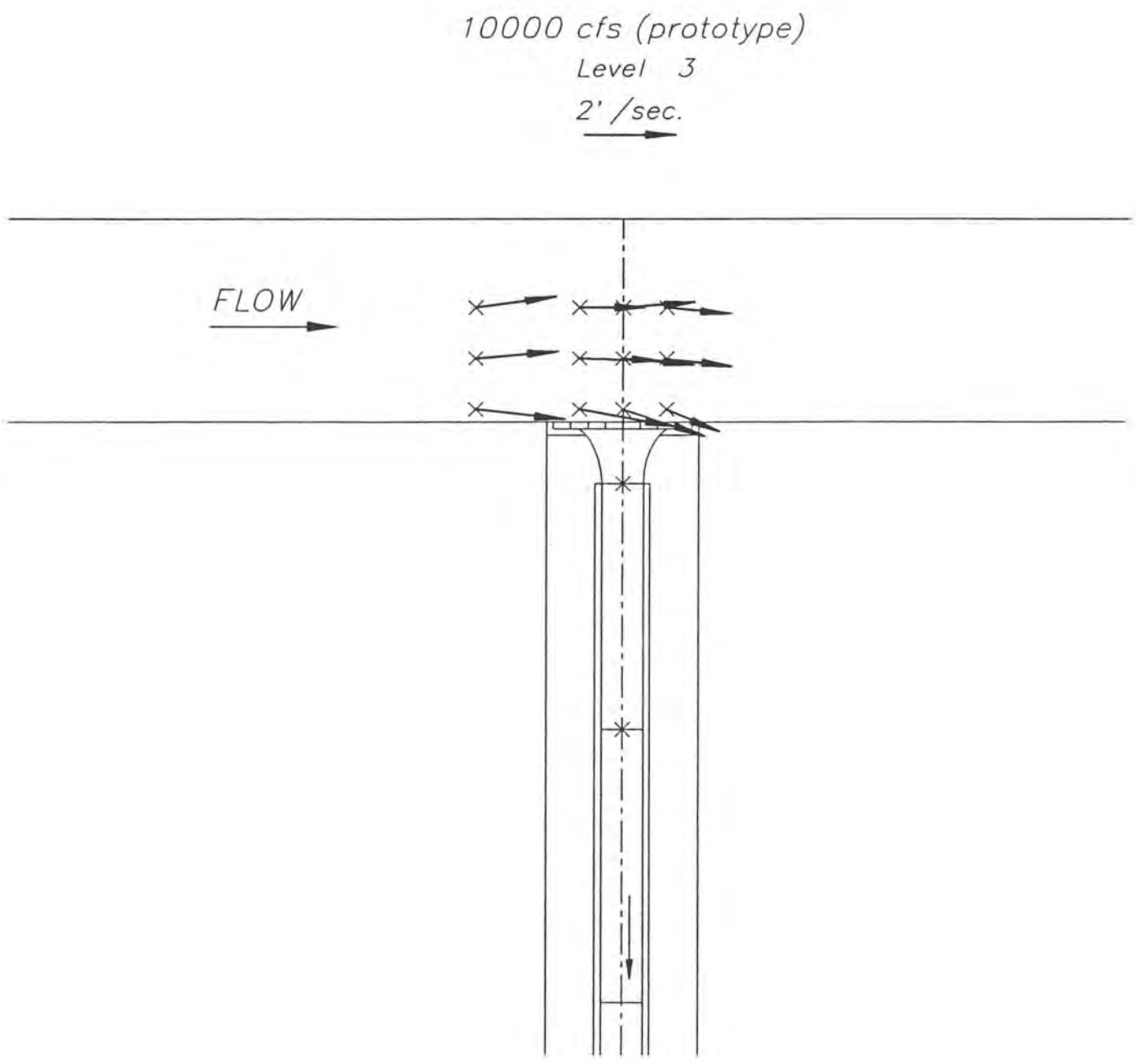

Figure 25 - Bypass entrance velocity vectors in X-Y plane measured 6.3 ft above the invert for 10,000 ft^3/s flow NIRG.

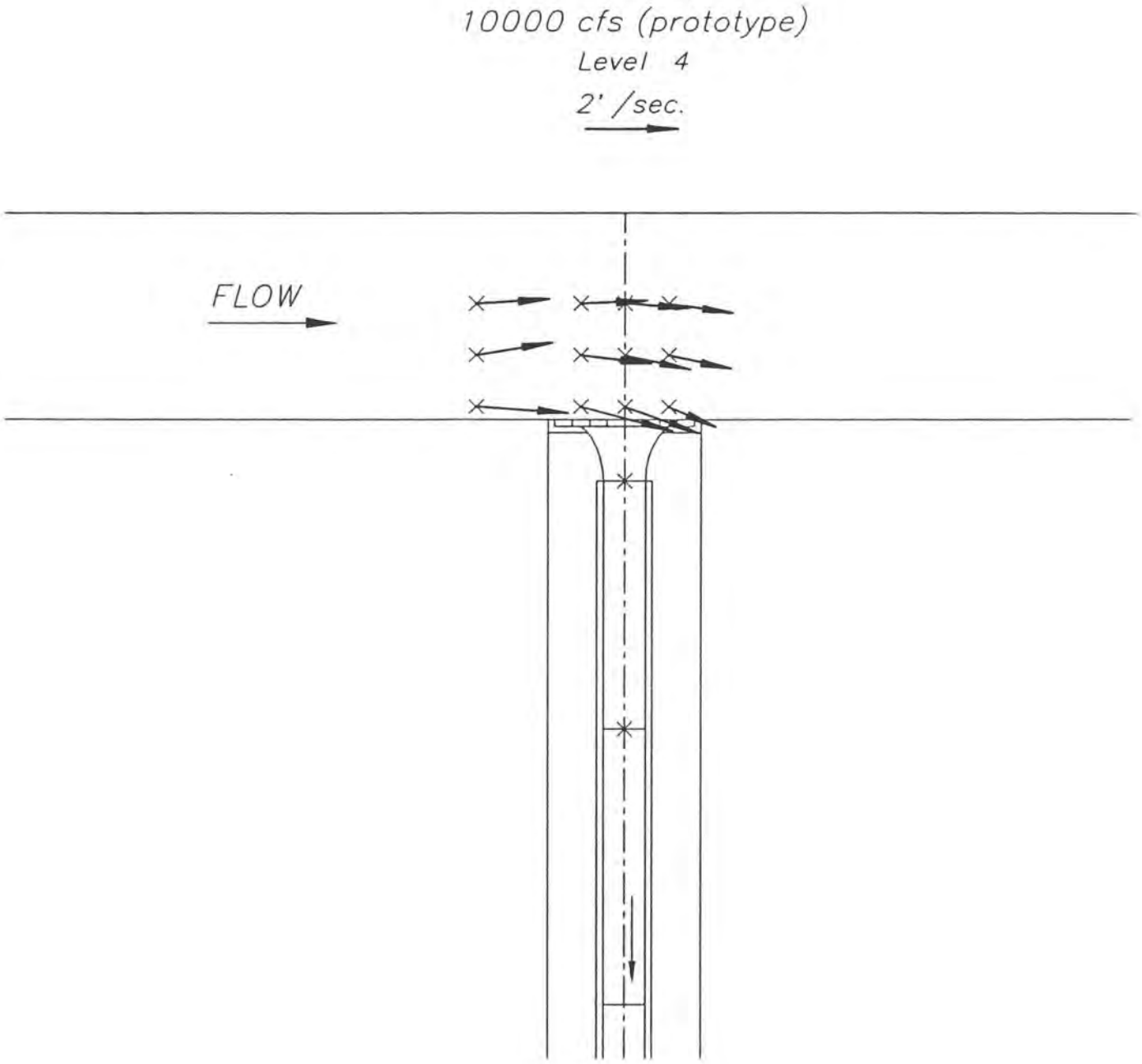

Figure 26 - Bypass entrance velocity vectors in X-Y plane measured 8.4 ft above the invert for 10,000 ft^3/s flow NIRG.

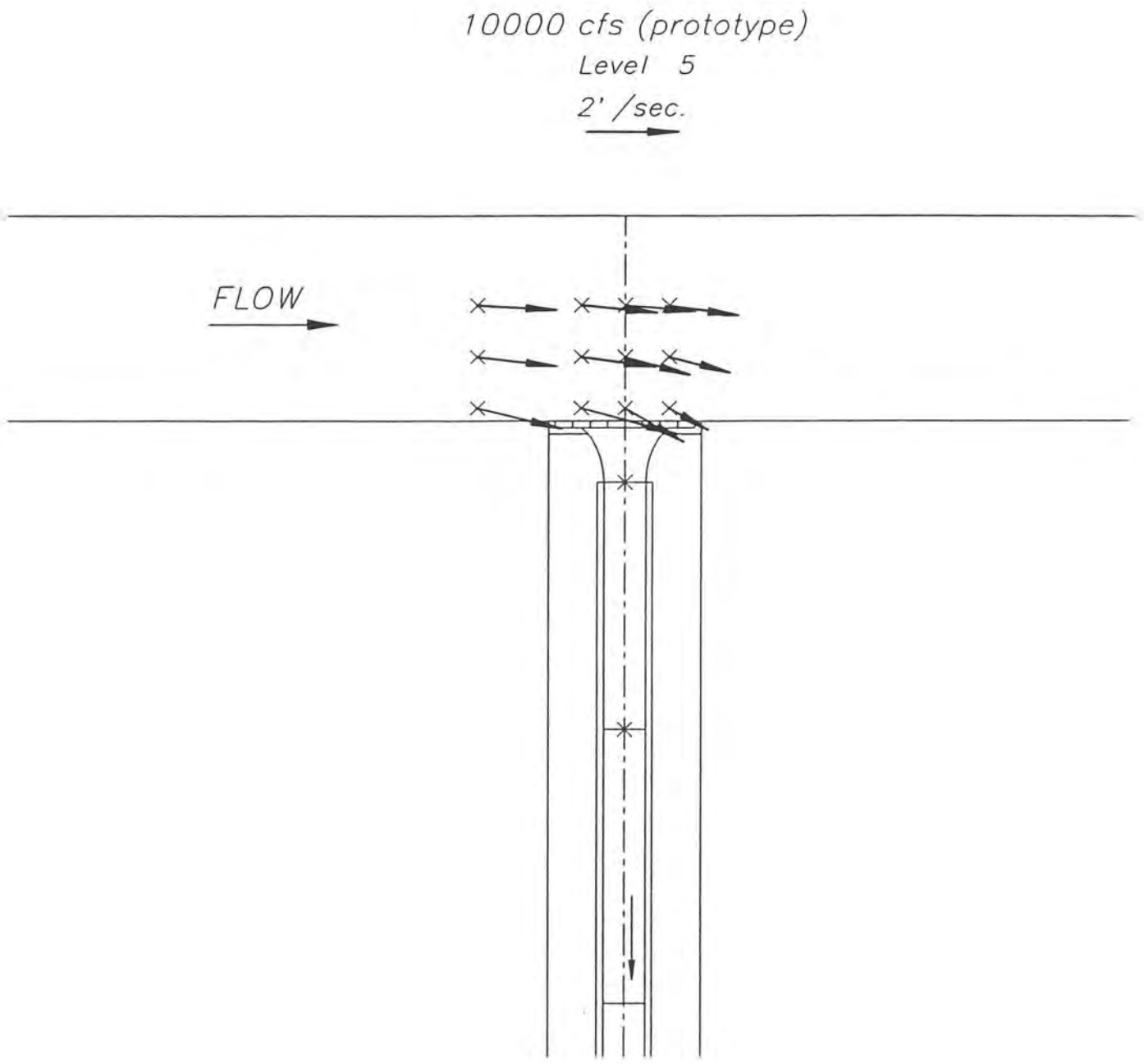

Figure 27 - Bypass entrance velocity vectors in X-Y plane measured 10.5 ft above the invert for 10,000 ft^3/s flow NIRG.

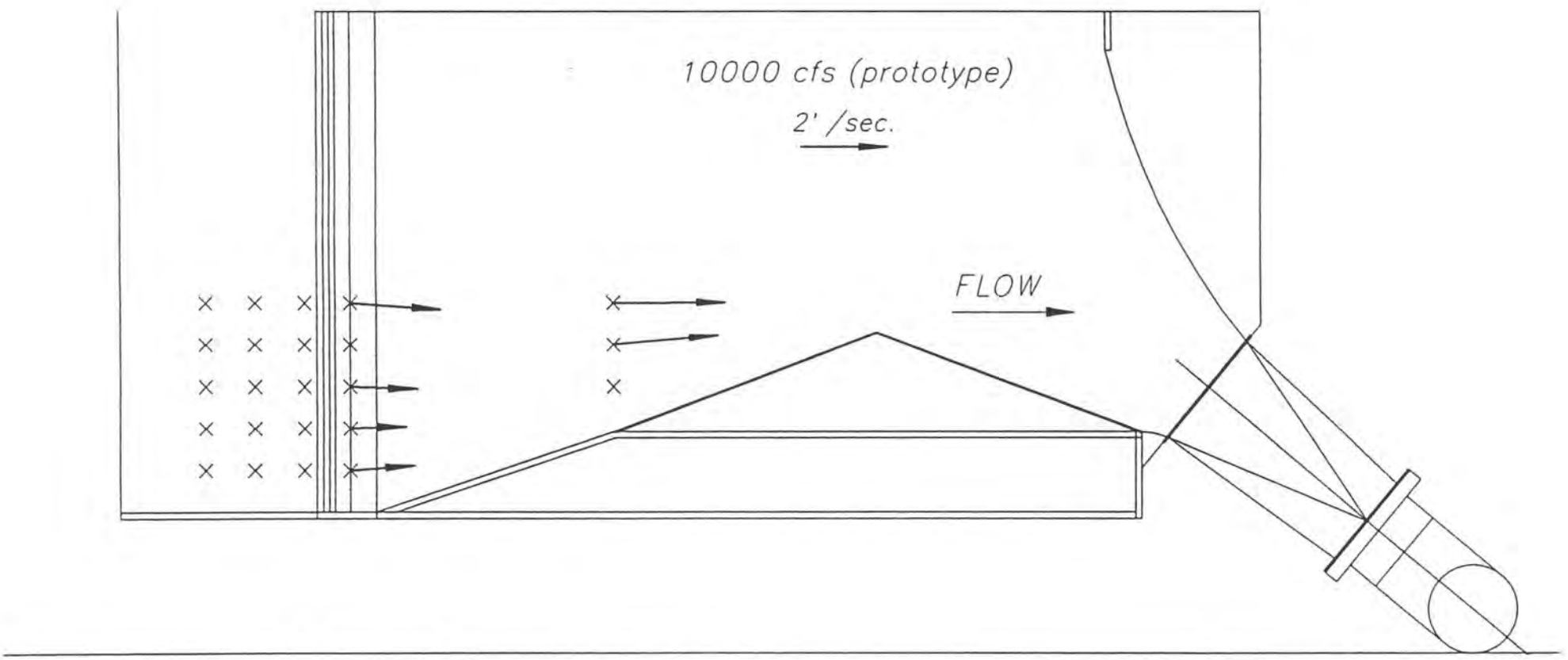

Figure 28 - Velocity vectors in X-Z plane measured in the bypass throat for 10,000 ft^3/s flow NIRG.

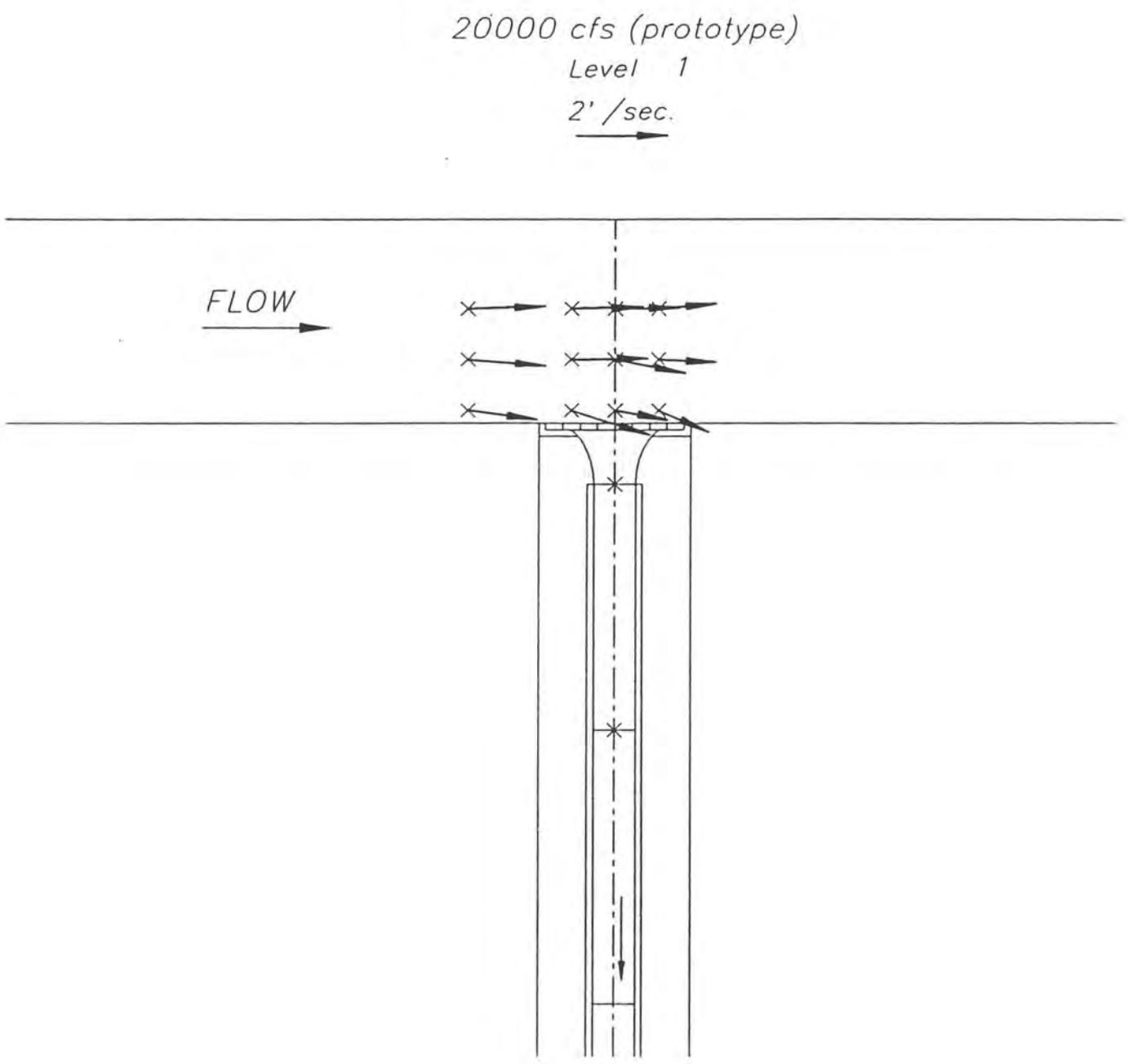

Figure 29 - Bypass entrance velocity vectors in X-Y plane measured 2.1 ft above the invert for 20,000 ft^3/s flow NIRG.

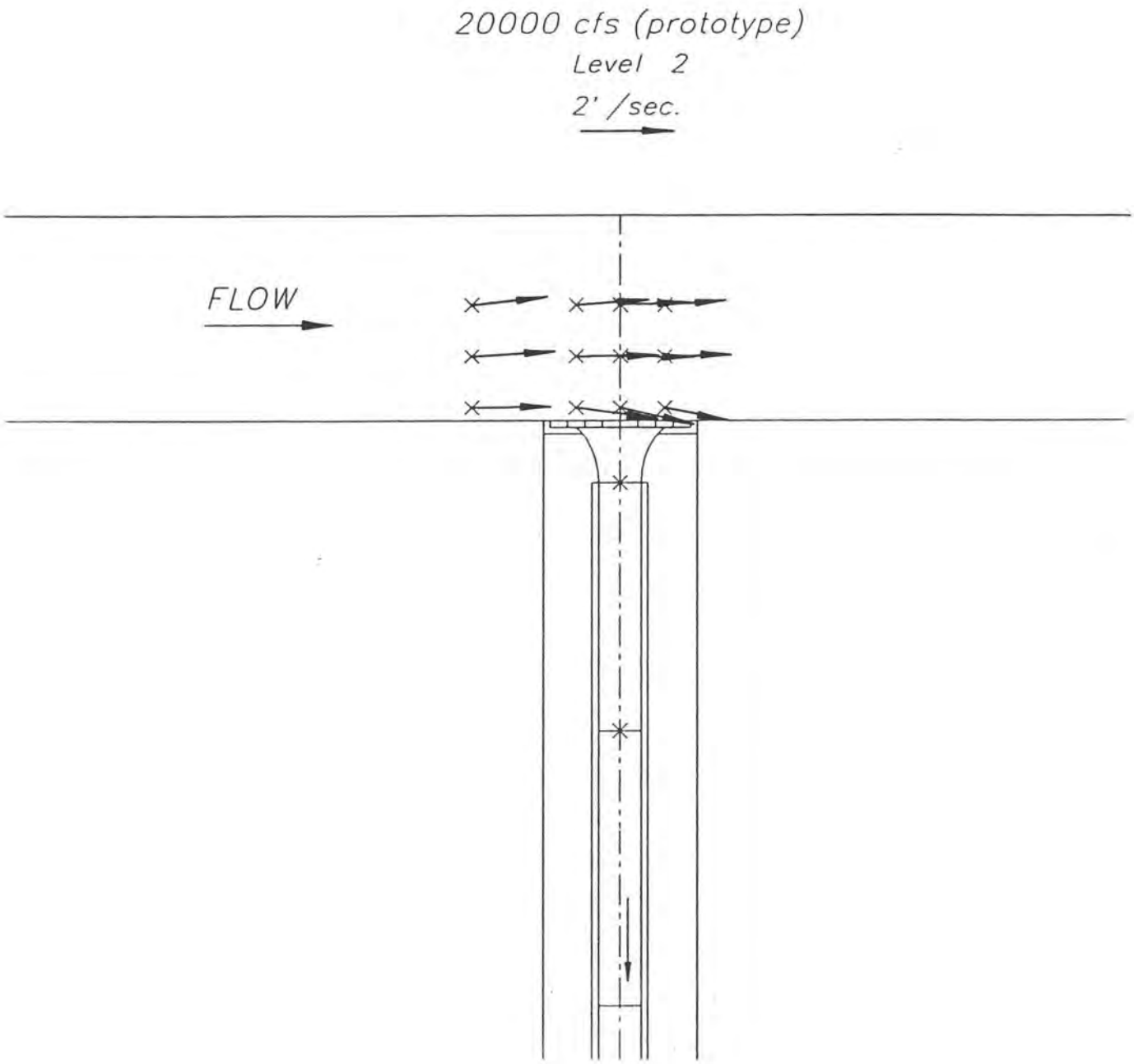

Figure 30 - Bypass entrance velocity vectors in X-Y plane measured 4.2 ft above the invert for 20,000 ft^3/s flow NIRG.

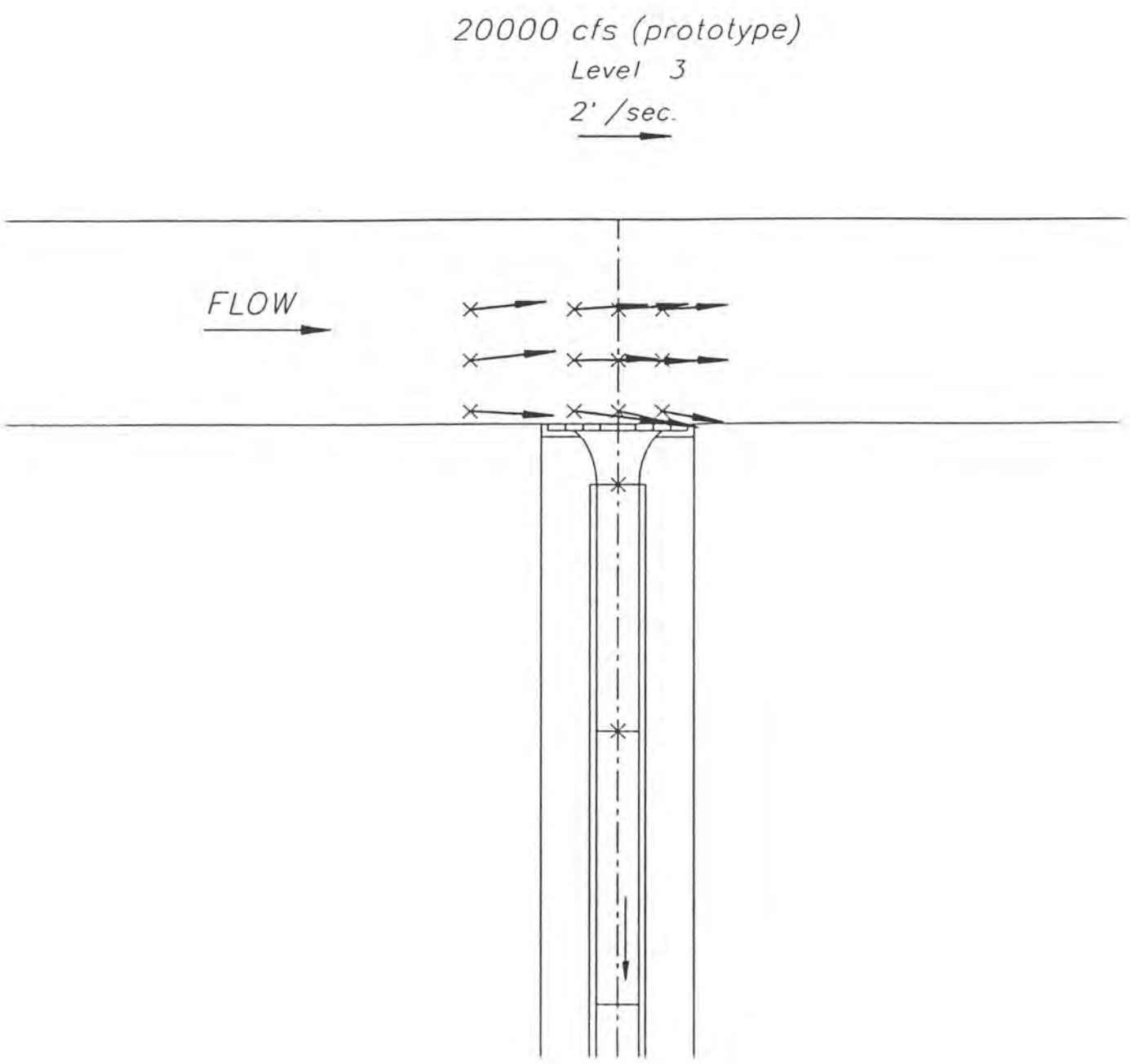

Figure 31 - Bypass entrance velocity vectors in X-Y plane measured 6.3 ft above the invert for 20,000 ft^3/s flow NIRG.

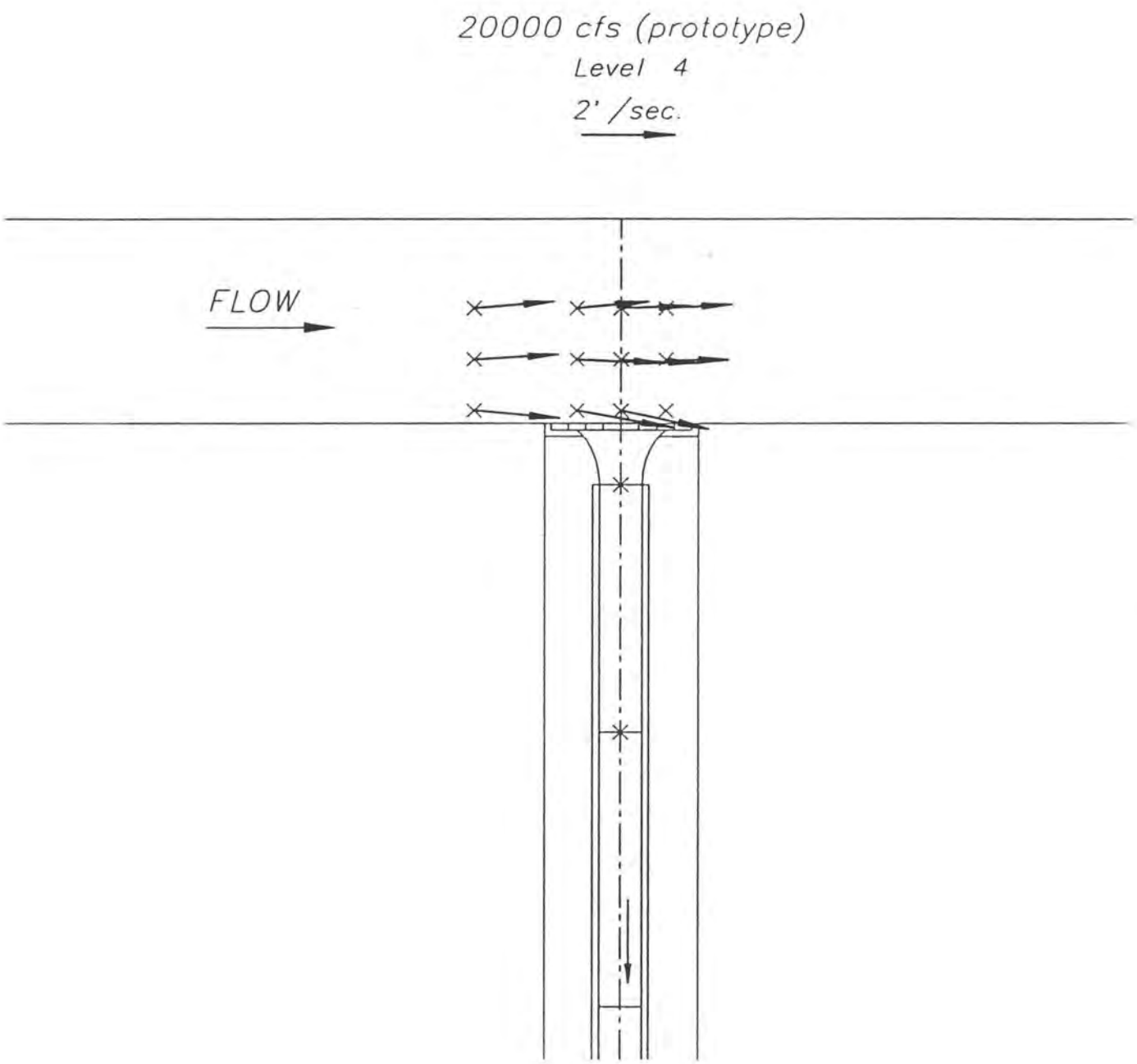

Figure 32 - Bypass entrance velocity vectors in the X-Y plane measured 8.4 ft above the invert for 20,000 ft^3/s flow NIRG.

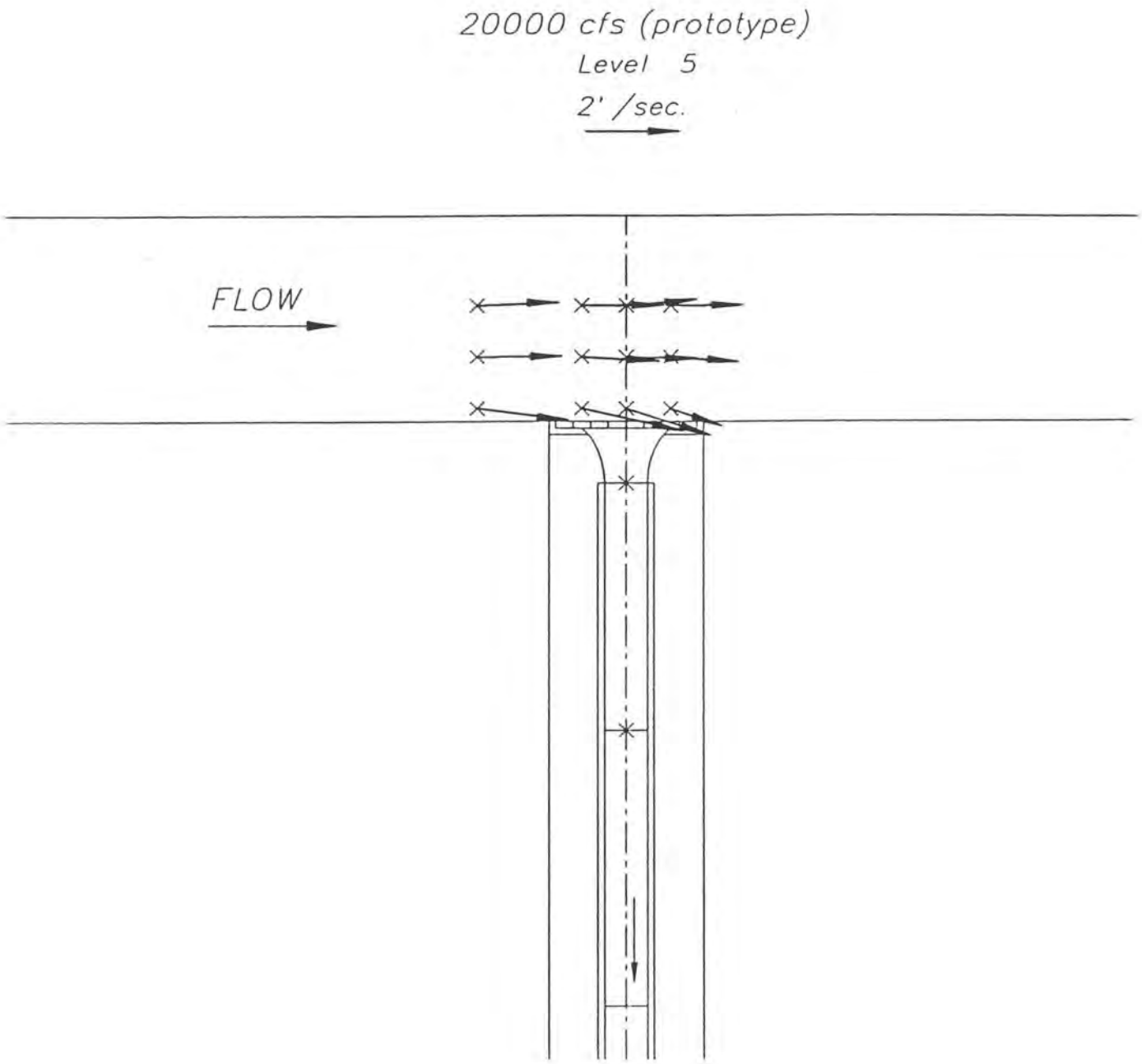

Figure 33 - Bypass entrance velocity vectors in the X-Y plane measured 10.5 ft above the invert for 20,000 ft^3/s flow NIRG.

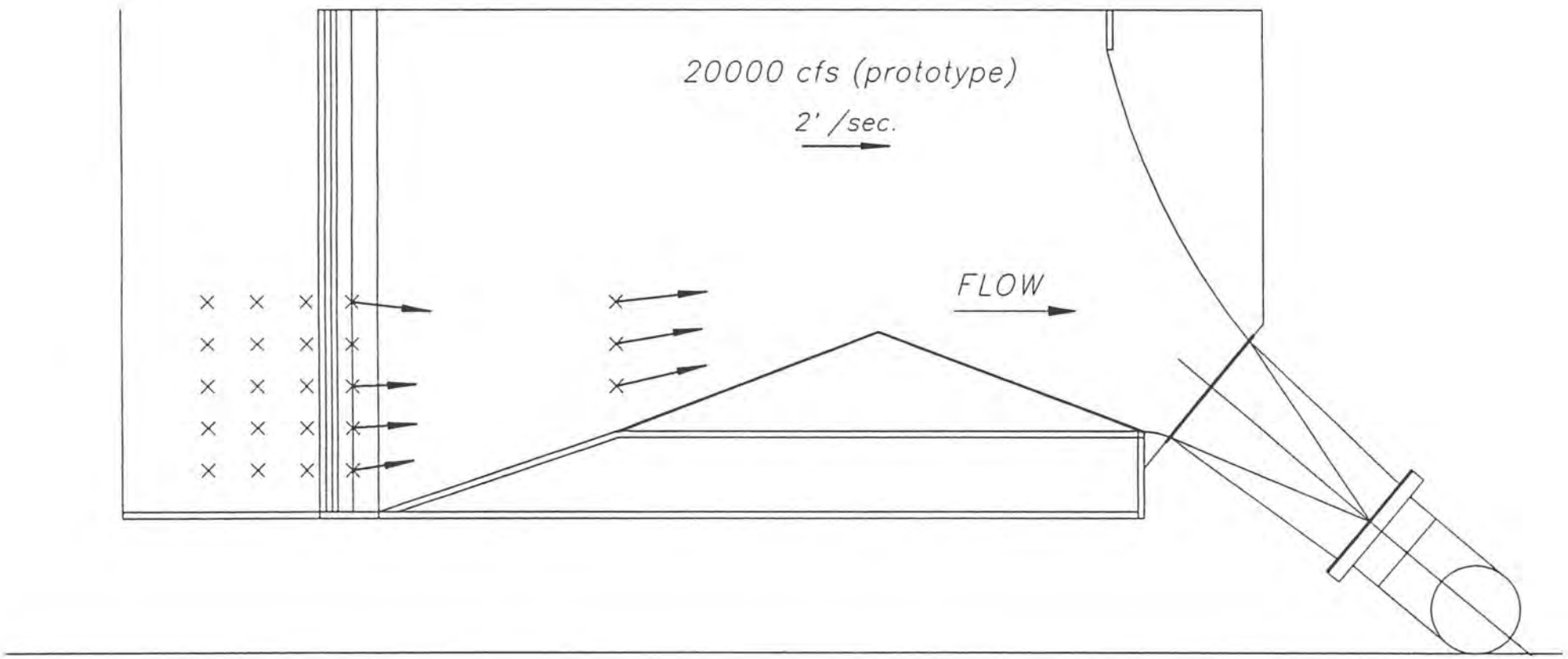

Figure 34 - Bypass velocity vectors in the X-Z plane measured in the bypass throat for 20,000 ft^3/s flow NIRG.

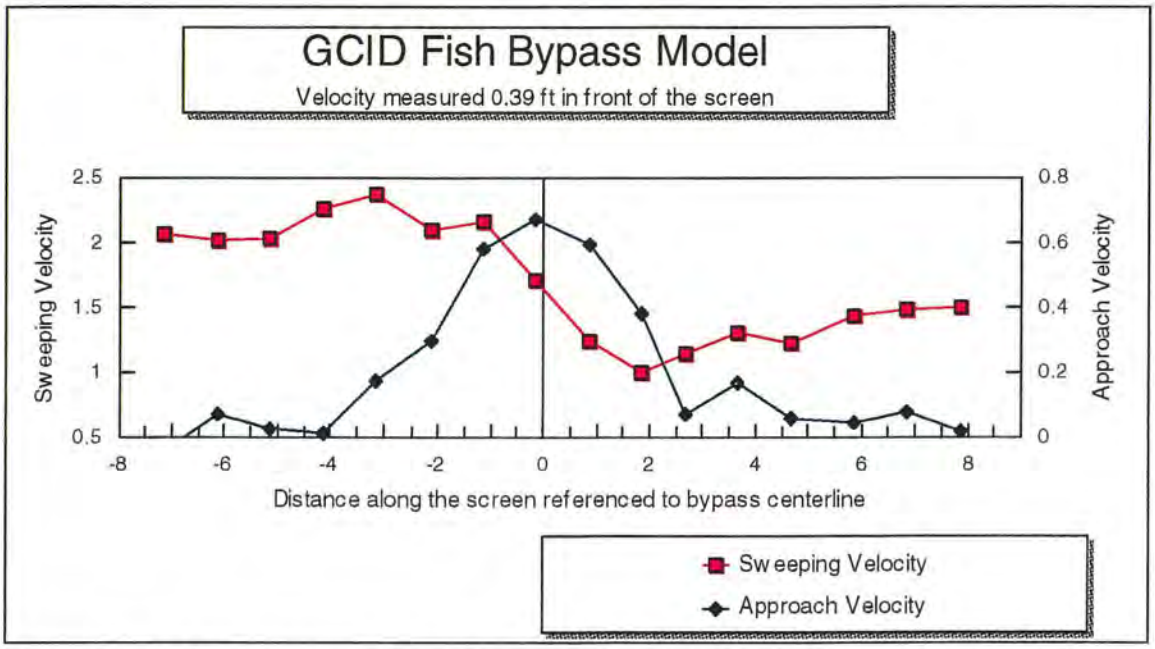

Figure 35 - Velocity traverse along the screen face crossing the bypass entrance, 1:5 scale bypass model.

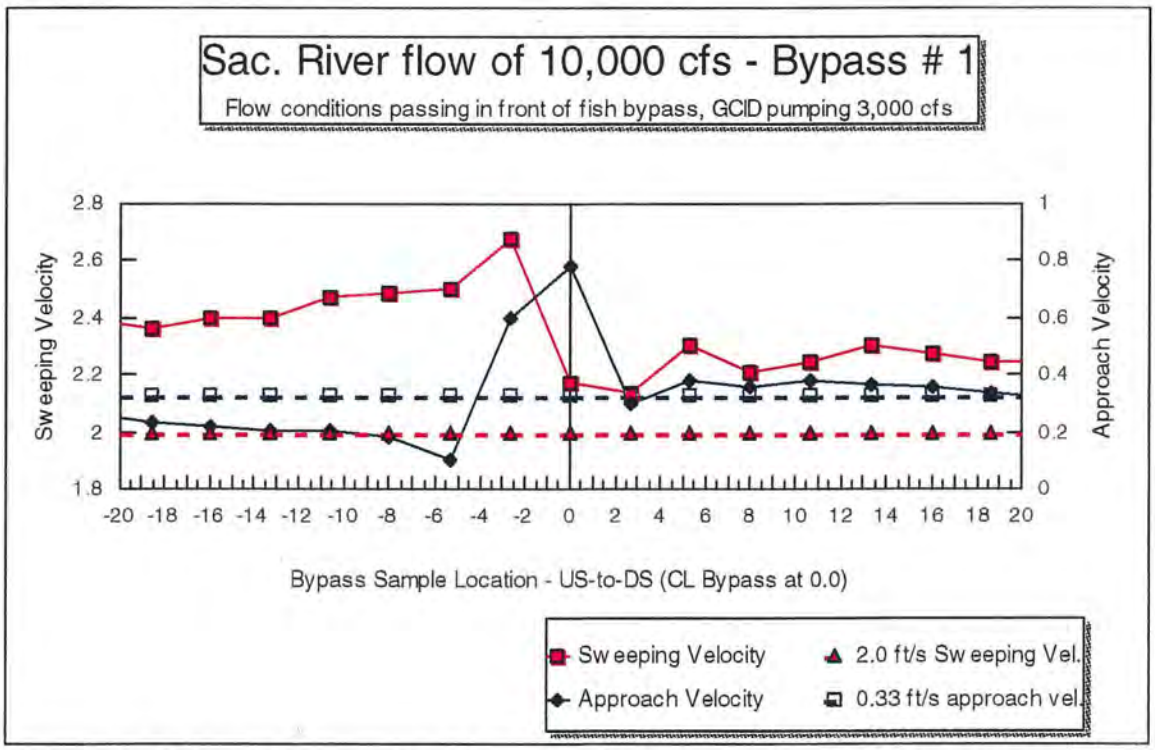

Figure 36 - Velocity traverse along the screen face crossing bypass #1 between screen bays 48 and 49, 1:16 scale screen model..

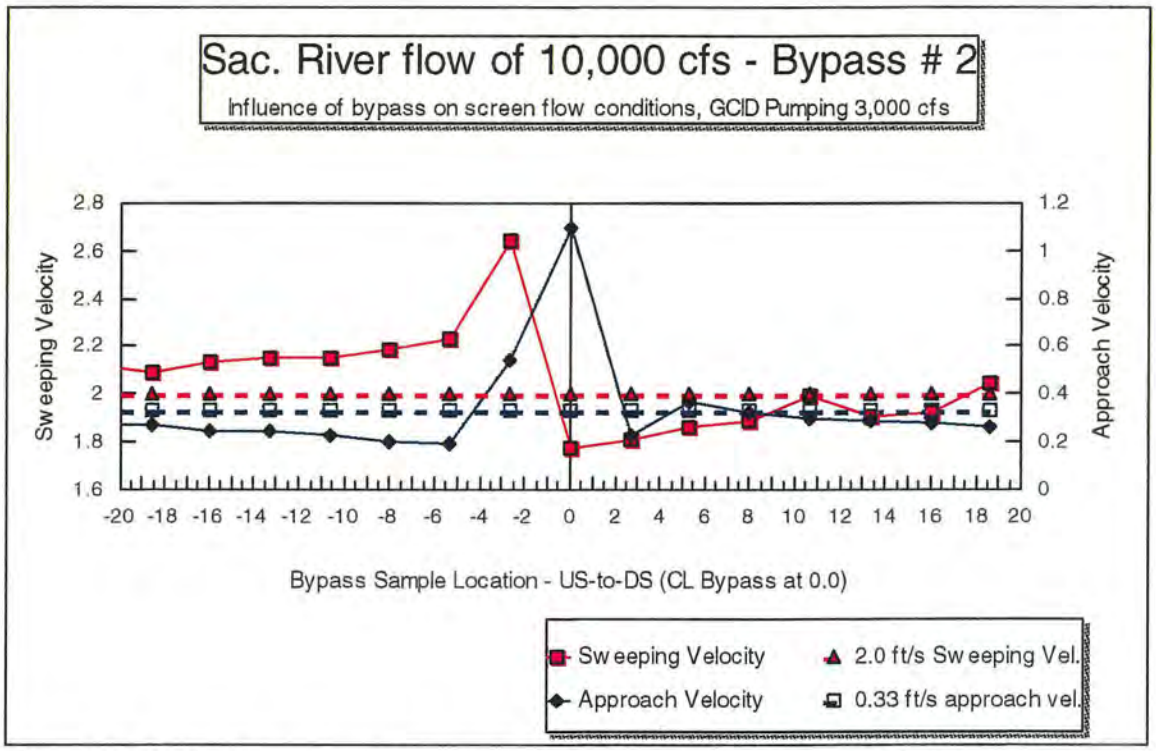

Figure 37 - Velocity traverse along the screen face crossing bypass #2 between screen bays 41 and 42, 1:16 scale screen model.

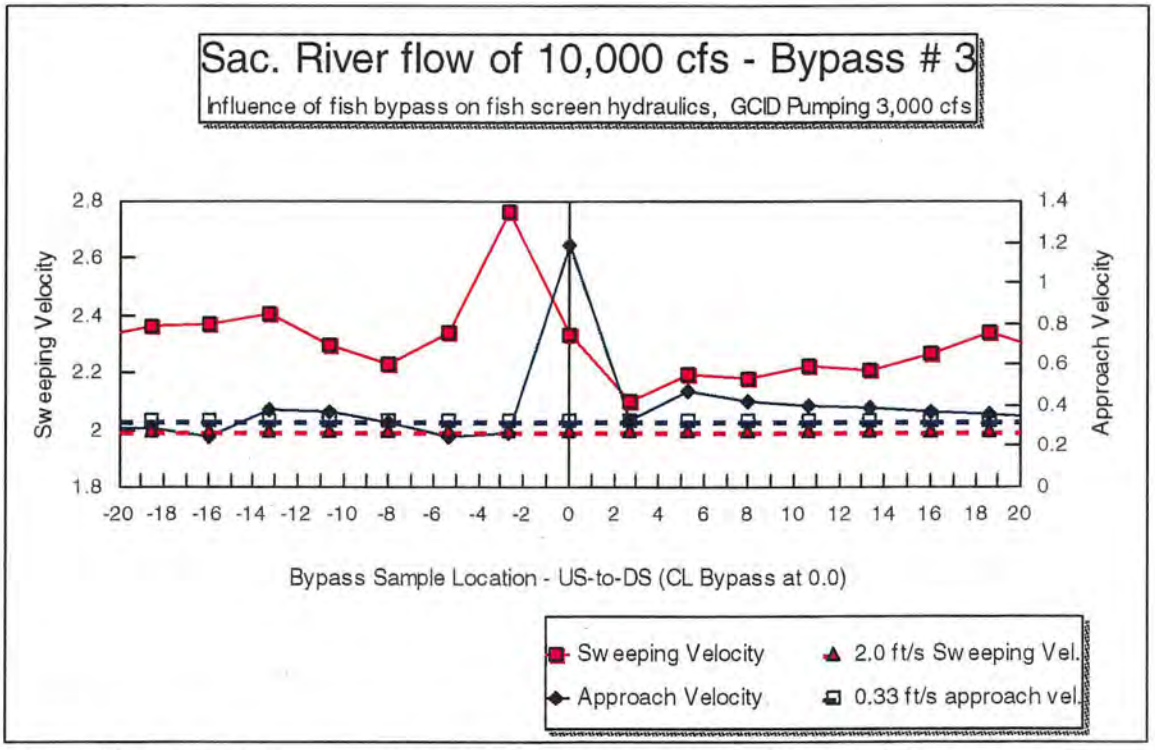

Figure 38 - Velocity traverse along the screen face crossing bypass #3 between screen bays 22 and 23, 1:16 scale screen model.